SSSU 1/78
ISSN 0140 3818

UNIVERSITY OF SOUTHAMPTON

DEPARTMENT OF SHIP SCIENCE

FACULTY OF ENGINEERING AND APPLIED SCIENCE

RUDDER DESIGN DATA FOR SMALL CRAFT

by

Dr. A.F. Molland

August 1978
Ship Science Report No. 1/78

RUDDER DESIGN DATA FOR SMALL CRAFT

A. F. Molland

August 1978

Ship Science Report No. 1 / 78.

SUMMARY

The purpose of this paper is to review available design data and provide a design procedure for the rudders of high performance small craft. While adequate background is presented to satisfy the user with a theoretical bias the needs of the practical designer are borne in mind and all the required data are presented in graphical form which does not require a full appreciation of the theoretical aspects for its use.

A design approach is outlined which basically employs free-stream data together with the relevant corrections for effective aspect ratio, inflow angle of attack and velocity.

Free-stream data applicable to the design of small craft all-movable and skeg rudders are presented and reviewed.

Applicable design criteria regarding speed, angle of attack and influences of proximity of hull to top of rudder are discussed; data relevant to surface effects as applied to transom rudders, or other types operating near the surface, are considered and the influence of free surface assessed.

The data are presented in non-dimensional form whereby comparisons between the various rudder types, or variation in parameters for a particular rudder type, can be made; some worked examples are included in appendices to illustrate the use of the data.

General conclusions are drawn from the available data and design recommendations made.

CONTENTS

NOMENCLATURE

A - Rudder Area

AR_E - Effective Aspect Ratio

AR_G - Geometric Aspect Ratio $(S/\bar{C})$ or (S^2/A)

C - Chord Length

$\bar{C}$ - Mean Chord Length

C_S - Skeg Chord

C_m - Movable Chord

C_R - Root Chord

C_T - Tip Chord

$CP_{\bar{c}}$ - Centre of Pressure, Chordwise, measured from leading edge

CP_s - Centre of pressure spanwise measured from root.

C_D - Drag Coefficient $(D/\frac{1}{2}\rho AV_R^2)$

C_{Do} - Minimum drag coefficient (at $\alpha = 0$)

C_L - Lift Coefficient $(L/\frac{1}{2}\rho AV^2_R)$

C_{Lmax} - Maximum Lift Coefficient

C_N - Normal Force Coefficient $(N/\frac{1}{2}\rho AV_R^2)$

C_m' - Moment Coefficient

C_R - Resultant Force Coefficient $(\sqrt{C_L^2 + C_D^2})$

C_{Dc} - Cross Flow Drag Coefficient

D - Drag Force

d - Diameter of Rudder Stock

F_c - Froude Number based on Rudder Chord $(V/\sqrt{g\bar{c}})$

F_s - Froude Number based on Rudder Span $(V/\sqrt{gS})$

G - Root gap

h - Immersion of top of Rudder

$\bar{h}$ - Immersion Factor (h/S)

k - Aspect Ratio Factor (AR_E/AR_G)

L - Lift Force

M - Bending moment about root of rudder or bearing $(R \times CP_s \times S)$

M_E - Equivalent bending moment

N - Force normal to Rudder

R - Resultant Force $(\sqrt{L^2 + D^2})$

R_n - Reynolds Number (based on Chord) $(V\bar{c}/\nu)$

S - Rudder Span

t - Rudder Section Thickness

t_{max} - Rudder Section Maximum Thickness

T - Torque about Rudder Stock ($N \times \bar{x}$)

T_E - Equivalent Torque

V_s - Boat Speed

V_R - Effective Speed Past Rudder

w_T - Wake Fraction

X - Induced Drag Factor

$\bar{x}$ - Distance of centre of pressure from Rudder Stock

α - Rudder Angle Relative to Flow

α_{stall} - Rudder Stall Angle

β - Skeg Angle relative to Flow

δ - Rudder Angle Relative to Skeg or Craft

Ω - Sweep of Quarter Chord

ρ - Mass Density (1025 kg/m^3 for salt water)

ν - Kinematic Viscosity (1.19×10^{-6} for salt water)

1.1 INTRODUCTION

1.1 General

The functions and operation of a rudder, which are reviewed briefly later, have been extensively described in published papers and books over the years and are generally well understood. However, the means of designing a rudder to fulfil the required functions are not necessarily well defined, nor the data which exists readily available to small craft designers.

Formulae such as those based simply on area and the square of speed for deriving the forces on a rudder, whilst providing reasonably satisfactory estimates in the past for ship rudders, omit to take account of other important variables and are often not suitable for small craft rudders.

Extensive data are available for a more scientific and systematic approach to rudder design and an attempt is therefore made to present applicable data, including those for skeg rudders which have gained in popularity in recent years. Data is presented relating to free surface effect (i.e. the absence of the hull surface between the rudder top and the water surface), since this can be a significant factor in the case of small craft. The various data are discussed and their applications illustrated by means of example calculations.

It is worth noting at this stage that, in considering the rudder design problem, two analysis situations exist. One concerns the need to compare alternative rudder designs or alternative parametric variations of a particular rudder type. In this case comparisons may be made, using some 'measure of merit' without necessarily evolving a precise final answer for the actual working rudder. The second use of design data is in estimating absolute values of rudder forces and moments whereby the actual rudder characteristics such as area and shape can be evolved and the stock size necessary to carry these forces calculated. It will be seen later that for most situations, available data makes possible the derivation of actual rudder characteristics. However, whilst general trends for the influence of free surface can be assessed, precise evaluation is not always possible.

1.2 Design Range

Data applicable to the design of rudders for small craft, both sail and power, up to a vessel length of about 30m are presented.

A typical range of speeds and resulting Reynold's and Froude numbers useful in the interpretation of the data in this paper is outlined in TABLE I.

A survey of rudders applied to this range of craft would indicate the principal rudder parameters to generally lie within the following ranges, and the data presented are generally acceptable for rudders designed within these limits :-

Effective Aspect Ratio	AR_E	2	to	6
Thickness Ratio	t/C	0.10	to	0.15
Taper Ratio	C_T/C_R	0.6	to	1.0
Reynolds Number (Rudder)	R_n	1×10^6	to	3×10^6

The rudder types considered are broadly grouped in the categories shown in Figure 1.

Rudders on fast craft may be subject to cavitation; this is however unlikely under about 25 knots for most aerofoil sectioned rudders. Above about 25 knots when cavitation might be possible, care must be taken in the choice of section type, e.g. possible use of wedge sections. This paper does not pursue further the subject of cavitation, but very useful design data and conclusions can be drawn from the pressure distributions available from Reference 1 and References 2 and 3.

1.3 Functions of Rudder

The functions of a rudder are outlined as follows :-

(a) to provide manoeuvrability, i.e. the ability to provide a yawing moment to the craft leading to the development of forces on the hull which cause it to turn.

(b) to provide directional stability, i.e. coursekeeping for power craft and sailing craft particularly when sailing off or down wind.

(c) to contribute to side force and hence resist leeway in the case of the sailing craft.

More detailed considerations of the requirements for the sailing craft rudder are discussed, for example, in References 4 and 5.

It should be noted that in fulfilling these functions, the rudder design requirements are likely to conflict. For example, a rudder which is designed for high efficiency in coursekeeping (say at relatively low angles of attack) will not necessarily be efficient at the higher angles of attack needed for manoeuvring. Similarly a sailing craft rudder working near optimum at low angle of attack to provide side force will not necessarily be the best to offer quick manoeuvring nor provide the high rudder forces required to control the craft in heavy seas, or whilst rolling or broaching.

A rudder will normally be designed to meet the requirements predominating for the particular craft in question. It follows from the foregoing comments however that compromise will have to be accepted in the design if, for example, satisfactory overall characteristics are required to be achieved.

The forces acting on a rudder, and the notation used in the presentation of data are shown in Figures 2, 3 and 4.

1.4 Design Approach

A typical overall approach to the design of a rudder may be summarised as in Figure 5. This follows a logical sequence and may be employed in its entirety, or component parts may be used individually. Iteration within particular steps of the path may be desirable before the choice of rudder parameters is finalised.

The overall design procedure basically requires the use of free-stream or open-water data (i.e. without the influence of hull or propeller) applicable to rudder configurations. Recourse can be made by the designer to relatively large quantities of published aerodynamic (and some hydrodynamic) free-stream information. The principal data available are for symmetrical section aerofoils of low aspect ratio and are suitable for many marine applications, e.g. References 6, 7 and 8. Reference 9 summarises in tabular form a lot of the available data.

The following five sections of this paper present and discuss available free-stream data applicable to the design of all-movable and skeg rudders. Further sections consider rudder area, applicable aspect ratio and modifications to inflow velocity and angle of attack.

2. ALL-MOVABLE RUDDER DATA

2.1 General

Whilst equations 1 - 11 (Appendix 1) define empirical fits to much of the data available, their use can be cumbersome and difficult for the practical designer, hence the data are also presented in a readily usable graphical form in Figures 6a to 6g.

The following comments are made on the interpretation of the data available and its presentation. Much of the theoretical treatment may be safely ignored by the reader with a non-mathematical background provided careful account is taken of the conclusions.

2.2 Lift

The lift curve for low aspect ratios is not strictly linear. Approximate theory assumes that the lift is composed of two parts, one arising from flow in the longitudinal plane and the other from the cross flow associated with low aspect ratio (discussed in more detail in Section 8.1).

Figure 6a (C_L - α), based on Equation 1 indicates the primary influence of aspect ratio on the lift characteristics.

Lift curve slope ($dC_L/d\alpha$), given by Equation 2 represents a satisfactory mean line for the available data; this assumes that the root gap is effectively zero in the reflection plane case (to be discussed later). The significance of thickness ratio (t/c) is small in the range t/c 0.10 to 0.15; for t/c 0.10 to 0.05 an average increase in ($dC_L/d\alpha$) of about 0.004 follows. Published data would indicate an insignificant influence on ($dC_L/d\alpha$) of taper ratio variations in the range 0.60 to 1.0, and sweep variations in the range $\pm$ 10°.

2.3 Drag

The total drag on a lifting surface of finite span is made up of two parts, one arising from friction and form effects (profile drag) and the other induced by the production of lift (induced drag). These two components are contained in Equation 5 which clearly shows that the induced component (XC_L^2/AR_E) increases as aspect ratio gets smaller. Based on an analysis of available free-stream data, a mean value for the induced drag factor X of X = 0.37 is proposed for all-movable rudders as being satisfactory for practical design purposes.

Figure 6e shows mean curves for minimum drag coefficient C_{Do} for various section thicknesses and Reynolds number; these curves were faired through data derived from Reference 1 and further experimental values such as References 8, 10, 11 and 12.

Whilst theoretical relationships exist between taper, sweep and induced drag, the data derived from model tests (e.g. Reference 8) is inconclusive. Similarly the influence of taper and sweep on C_{Do}, (References 8 and 9) is not conclusive, hence no attempt is made to account for these parameters in the presentation.

2.4 Stall Angle

The principal influence on stall angle (α_{stall}) is aspect ratio and this effect, for varying Reynolds Numbers, is shown in Figure 6c.

2.5 Maximum Lift Coefficient

The principal influences of Reynolds Number, thickness and aspect ratios are shown in Figure 6d.

2.6 Centre of Pressure

2.6.1 Chordwise $\bar{CP}_c$

A change in position of $\bar{CP}_c$ occurs with changing angle of attack, the amount of movement becoming larger as aspect ratio is decreased. As angle of attack is increased $\bar{CP}_c$ moves gradually aft, with relatively rapid movement aft as stall is approached. The position and movement of $\bar{CP}_c$ may be deduced from Equations 8, 9 and 10.

In relation to rudder design for small craft the forwardmost position of $\bar{CP}_c$ (as $\alpha \to 0$) and its position at stall are the most important characteristics, and these two positions for different aspect ratios are shown in Figure 6f.

The forwardmost position shown in Figure 6f is a satisfactory approximation to the available data and can be represented by Equation 10.

$$\text{i.e. Since } C'_m = \frac{N.CP\bar{c}}{\frac{1}{2}\rho AV^2\bar{c}} = \frac{N}{\frac{1}{2}\rho AV^2} \times \frac{CP\bar{c}}{\bar{c}}$$

$$= C_N \times \frac{CP\bar{c}}{\bar{c}}$$

as $\alpha \to 0$, $C_N \to C_L$

$$\therefore C'_m \simeq C_L \times \frac{CP\bar{c}}{\bar{c}}$$

$$\text{and } \frac{CP\bar{c}}{\bar{c}} \simeq \frac{C'_m}{C_L} \simeq \left(\frac{dC'_m}{dC_L}\right)_{\alpha = 0} = C_L$$

Whilst available data indicates a movement of $CP\bar{c}$ forward by about 1% for taper ratio of 0.60 and aft by about 1% for a taper ratio of 1.0, the scatter of data is generally as large as this (up to ± 1%); further, variation due to thickness ratio and sweep (say ± 10°) tend to lie within this scatter.

$CP\bar{c}$ at stall, shown in Figure 6f, represents a mean curve through all the data; no specific trends were deduced for the influence of thickness, taper and sweep.

The position of $CP\bar{c}$ at stall, in conjunction with the maximum normal force, is used to deduce the maximum torque on rudder stock.

The forwardmost position of $CP\bar{c}$ is important in that the stock must be located forward of this $CP\bar{c}$ position if negative torques are to be avoided and satisfactory rudder free-trailing characteristics are to be achieved. It should be noted that the forwardmost position moves forward as aspect ratio is decreased, and can be considerably further forward than the 25% normally associated with high aspect ratio foils. Locating the stock about 5%$\bar{c}$ forward of forwardmost $CP\bar{c}$ position would appear to be a satisfactory compromise (i.e. about 12%$\bar{c}$ to 17%$\bar{c}$ aft of leading edge as aspect ratio varies from 2 to 6, (see Figure 6f); this provides reasonable balance for the all-movable rudder whilst retaining positive torque as $\alpha \to 0$, and provides 'feel' in the case of the hand held all-movable rudder.

2.6.2 Spanwise CP_s

The centre of pressure spanwise tends to move down rudder (from 3% of S to 7% of S) as angle of attack is increased, reaching

its final position at stall. CP_s at stall forms the most important design condition in respect of deducing maximum bending moment and hence strength criteria; the position of CP_s at stall, for variation in aspect ratio and taper are shown in Figure 6g. Data for these curves were derived from free stream sources such as References 8 and 12.

3. SECTION SHAPE

Extensive discussion often centres around the subject of section shape. The principal design factor is thickness, the minimum requirements for which will be governed by structural needs. Actual thickness will be governed by hydrodynamic requirements since thickness change will affect the minimum drag, separation tendencies and hence stall angle and maximum lift coefficient. The distribution of the thickness chordwise, and the position of maximum thickness also has an influence on these characteristics. Reference 1 presents test data for a wide range of shapes; it should be emphasised that these results are for two-dimensional sections (or infinite aspect ratio) and would require correction to actual aspect ratio employed. Analysis of the data for different section shapes yields a general trend. For example, the 'normal' aerofoil shape (e.g. N.A.C.A. 00 series with maximum thickness 30% aft of leading edge) has very satisfactory characteristics for movable control surfaces such as rudders. 'Low drag' shapes (such as the N.A.C.A. 65 or 66 series with maximum thickness 45% - 50% aft) have lower drag coefficients at low angles of attack (up to approx. 3^{o}) yielding what is termed a drag bucket. These 'low drag' forms with maximum thickness further aft do however exhibit earlier separation tendencies with increase in angle of attack with consequent increase in form drag and earlier stall; since there is no significant difference in the induced drag at a given lift for the section shapes being discussed this leads to higher drag for the 'low drag' shape at higher angles of attack. A comparison between these principal characteristics for the 'normal' and 'low drag' forms is shown diagrammatically in Figure 7. It should be added that the data in Reference 1 indicates that the drag bucket is only achieved for very smooth sections, and that the presence of even minimal roughness will eliminate this drag bucket effect.

The overall results suggest that the low drag forms are possibly suitable for applications with limited range requirements for angle of attack (e.g. keels) when the benefits of the drag bucket might be utilised, whilst the normal aerofoil shapes are more suitable for movable appendages such as rudders which require efficient operation over a larger range of angles.

The N.A.C.A. 00 series is well proven both for small craft and large ship rudders; a further consideration is that its maximum thickness at 30% aft of leading edge satisfies the typical area of location of rudder stock. Offsets for this section (as a percentage of maximum thickness) are given in Figure 8.

The trailing edge thickness of aerfoil sections (which have been primarily evolved for aircraft use) is generally too small for marine applications. Typical methods of increasing thickness to practical values (e.g. 1 to 3 mm say in the case of small craft) are to thicken the trailing edge locally and fair in, or remove the last 1½% to 3% of section to attain adequate thickness. Thickening the trailing edge for practical reasons by this order of magnitude has a small influence on drag and can in fact lead to small increase in maximum lift (Reference 13)

4. TIP SHAPE

The presentation of the data in this paper is for square tips.

Some idea of the results of using faired tips for rudders is given in Reference 8 where, as an alternative to square tips, faired tips (approximating to a semi-circle) were tested. These alternative tip shapes are shown in Figure 4. Use of faired tips would indicate a small saving in drag to be made at low angles of attack, for example, using the results of Reference 8 there is a decrease in C_{Do} of up to 0.001 which can amount to up to 10% decrease in minimum rudder drag at $\alpha = 0$. At L/D max., C_D is decreased by about 5% and L/D increased by about 3%; at 10^o the L/D ratios are about the same and above 10^o the faired tip L/D is less than the L/D for the square tip case. Further, for the faired tip, stall angle is reduced by about 2^o and C_{Lmax} reduced by 0.02 to 0.10.

Hoerner, Reference 13, reports a small decrease in C_{Do} with rounded tips compared with square tips. Data presented in Figure 10 of that reference for lift against drag indicate no difference at low angles of attack and significant losses by the faired tip at larger angles of attack, which leads Hoerner to conclude that shapes having square tips are generally the ones exhibiting the least drag due to lift. The choice of tip shape therefore might well depend on whether ultimate rudder drag reduction at very small angles of attack is required or whether square tips are used for maintaining large rudder angle performance for manoeuvring or resisting broaching. The evidence available does however suggest that by using a square tip on the rudder, which lends itself to accurate and easy production, the hydrodynamic losses, if any, at low angles of attack are small compared with the gains to be made at higher angles of attack.

5. SKEG-RUDDER DATA

5.1 General

Data for skeg type rudders is very limited, and recourse normally has to be made to flapped foil data treating the flap as the movable rudder and the 'rudder' as the skeg; a restriction on such data is that the flap/total chord ratio is often lower than that suitable for skeg rudders. References 11, 14, 15 and 16 offer some help in evolving applicable characteristics.

5.2 Lift and Drag

Data for movable rudder area/total area (A_m/A_T) of 40%, 50% and 60% cross plotted from data in Reference 11 is shown in Figures 9a - c, (the 60% flap case is for a flap with 18% balance, since the zero balance case was not tested. However, a comparison between the results for the 50% case with and without balance indicate very small differences in lift and drag for small skeg angles; the 60% results are therefore assumed satisfactory for comparative purposes). An extrapolation for A_m/A_T of 70% and $AR_E = 4$ based on Figure 13 (discussed later), all-movable data and skeg data (References 13, 14 and 15) is given in Figure 10.

Figure 11 compares the lift coefficients and lift / drag ratios for the all-movable and skeg rudders (for $\beta = 0$); it is seen that whilst the rate of increase of lift is considerably less for the skeg rudder, its stall angle is delayed (by about 10^o) and the maximum lift coefficient achieved is about the same as the all-movable. However, the lift / drag ratio (i.e. measure of efficiency) for the skeg rudder is appreciably less than the all-movable. In other words, for the same developed lift at a particular angle, there is a significant increase in drag over the all-movable rudder. An outline calculation example is contained in Appendix 2 to illustrate the magnitude of these differences.

Figure 12 gives a further indication of the drag penalty incurred by the skeg rudder. Whilst the increase in drag with increasing angle of attack is primarily due to early separation of the flow over the movable part of the rudder (profile drag), it is assumed for comparative purposes to be a function of C_L^2 and hence can be included in the induced drag component. C_{Do} is assumed to remain approximately constant at about 0.016 for $\beta = 0$ and 0.025 for $\beta = \pm 5^o$ for these skeg rudders (compared with about 0.013 for the equivalent all-movable rudder). These curves in Figure 12 were derived from Figure 9b and c and clearly show that as skeg size is increased, there is a marked increase in induced

drag factor X (Equation 5), and hence induced drag; e.g. with a movable chord 60% of total, the induced drag factor X has increased to 0.78 (for $\beta = 0$) compared with about 0.37 for the all-movable case. There is a further increase in X with negative skeg angle β, but a slight improvement with positive β. The curves indicate a relatively rapid increase in X as movable chord is decreased below about 70%

Figure 13 gives the relationship between the lift on a skeg rudder (movable part plus skeg) in the region of 10° of helm, relative to the lift on an all-movable equivalent (L_s/L) and the movable area ratio (A_m/A_T). Various data have been included, and a design mean curve suggested. It should be noted that the high data is for two dimensional (infinite aspect ratio) sections with the gap between rudder skeg sealed. The lower results, from Reference 11, are probably accounted for by the relatively large gap required to allow for experiments on flap balance.

Figure 13 indicates that if gap size between rudder and skeg can be minimised an improvement in lift production follows. At the same time it is seen that even with the gap sealed the skeg rudder still falls short of the rate of increase of lift attainable by the all-movable rudder.

If the skeg rudder is considered as a total movable plus skeg combination, then it is not unreasonable to assume that the influences of overall rudder shape, section and tip shape discussed for the all-movable rudder, will also apply to skeg rudders.

5.3 Torque

In order to estimate torque and hence stock size for the skeg rudder the proportion of load carried by the movable part, together with its centre of pressure, is required. Figure 14, derived from the pressure distributions in References 15 and 16, offers guidance for these characteristics; typical examples of these pressure distributions are shown in Figure 15. A comparison is made with the simple assumption that the dotted distribution in Figure 15 is equivalent to the actual distribution. This suggestion was made, for example, by Jaeger (Reference 17). Using this assumption it is found that

$$L_m = \frac{C_m}{2\,C_s + C_m} \times L_T$$

(where L_m is the lift on the movable part and L_T is the total lift)

This relationship is included in Figure 14 and it is seen that whilst it errs a little on the high (safe) side for the higher C_m/C ratio, it should

prove satisfactory for general design purposes.

Analysis of the pressure data in References 15 and 16 indicated that, for both the 0.50 and 0.80 C_m/C ratios, the chordwise centre of pressure is approximately 33% of movable chord aft of stock as $\delta \to 0$, moving to approximately 40% aft of stock for $\delta = 20^o$ to 30^o, which should cover most small craft stall angles.

5.4 Design Procedure

Since the amount of skeg data is limited, and all-movable rudder characteristics relatively well defined, the proposed design procedure is to relate the rudder plus skeg characteristics (for a particular skeg size), to the all-movable configuration by means of Figure 13. Having estimated the total (rudder plus skeg) force from Figure 13, the lift on the movable portion together with its centre of pressure chordwise can be obtained from Figure 14. The centre of pressure spanwise is assumed to be in the same position as the equivalent all-movable rudder.

In the absence of drag data for the movable part alone, or for movable plus skeg combination for $C_m/C > 0.6$ (Figures 9 and 12), it may be assumed that the maximum lift force is equivalent to the maximum normal force for torque and bending moment calculations. An example illustrating this design procedure is given in Appendix 3.

5.5 Example Calculations and Discussion

Appendix 2 shows an example calculation comparing skeg and all-movable rudders for $\beta = 0$ and $\beta = +5^o$ at an assumed design condition, It is seen that appreciable drag increase is incurred by the skeg rudder, amounting to about 60% when $\beta = 0$ and 50% when $\beta = +5^o$.

However, when altering course from a position of $\beta = +5^o$ the all-movable rudder would need an 'instantaneous' helm movement of approximately 7^o to reverse the sideforce on the rudder whilst, for instantaneous reversal, the angle of attack on the skeg of the skeg-rudder is now -5^o and (from Figure 9c) rudder helm is required to be moved from $+4.5^o$ to -6^o (total 10.5^o) before the side force is reversed. This is clearly an undesirable characteristic.

The influence of negative angle of attack on the skeg is more pronounced as drift angle is developed; e.g. at a drift angle of say -10^o the all-movable rudder would require a helm angle of 17^o to give a net effective α of 7^o for the development of say $C_L = 0.33$ at max L/D of 11.

However, at $\beta = -10^{o}$ the skeg rudder requires a helm δ of about 23^{o} to develop $C_L = 0.33$ with a C_D of about 0.07 and hence L/D of 4.7.

These calculations indicate that the skeg rudder is less efficient than the all-movable equivalent, even when the skeg rudder is working near its ideal efficiency. Minimising or, better still, effectively sealing the gap between skeg and rudder will show a marked improvement in performance although, as shown in Figure 13, it will never achieve the same performance as the all-movable rudder. When manoeuvring the calculations indicate that the skeg rudder is even less efficient with a much lower rate of response and with the added penalty of higher drag.

The outline calculations effectively illustrate the reasons for the reported poor manoeuvring characteristics exhibited by skeg rudders. If the calculations were repeated with a rudder / skeg ratio of 50% the effect would of course be worse. Conversely if the movable part were increased to say 70% of total, improvements would be made and the differences in rudder types would be less drastic.

Broad conclusions to be drawn are that whilst the skeg rudder will not achieve the same hydrodynamic efficiency as the all-movable rudder in any conditions, its performance for power craft or sail craft when beating or running can be reasonably satisfactory, providing its skeg length does not exceed about 30% of $/^{total}_{mean}$ chord; further improvements follow if its skeg / rudder gap is sealed with say feathered strips. The fixed skeg does contribute to directional stability for the 'rudder free' condition, which may be a desirable feature for some sailing craft. Skeg rudder manoeuvring characteristics are however much worse and skeg length should, again, not exceed about 30% of $/^{total}_{mean}$ chord if satisfactory manoeuvring performance is to be achieved.

6. SEMI-BALANCED SKEG RUDDERS

This is a special case of the skeg rudder, as shown in Figure 1. This type has become very popular for large ships, and has recently been seen applied to sailing craft. It has presumably been applied to small craft for different reasons since a lower pintle (fundamental to its design concept for ships) has not been used.

A formal design approach for this rudder type has not yet been formulated. However, based on Reference 12, the following observations concerning their design can be made.

An approximate design approach is to treat the upper and lower portions of the rudder as a skeg rudder part and all-movable part, utilising the data available for these two rudder types.

The lower part of the rudder tends to act like a low aspect ratio all movable foil, hence its $\bar{CPc}$ may be as far forward as 10-15% aft of leading edge. Care therefore has to be exercised in the case of small craft whereby the rudder is not overbalanced. Available data would indicate that the ratio (movable area forward of rudder stock / total movable area) should not exceed about 15%

The centre of pressure of the movable part is lower than the all movable equivalent, but the total force on the movable part is reduced compared with the all-movable rudder, hence the root bending moment on the stock remains approximately constant.

The experiments reported in References 12 have been extended by sealing the gap between rudder and skeg. A significant improvement in lift was recorded, confirming the usefulness of the feathered sealing strips used by some designers.

7. RUDDER AREA

Rudder area for a particular rudder type may be calculated if, for example, the required yawing moment to provide a defined steering response is known. Similarly it may be calculated in the case of sailing craft if a known contribution to the side force from the rudder is required, or total theoretical balance equations are established as, for example, in Reference 18.

However, for most design situations the required force cannot be derived in a well defined manner, and rudder area is usually estimated from empirical data for similar vessels. In using such data it is important to confirm, where possible, that the base designs had adequate steering and directional stability qualities. Figure 16 offers some guidance for a preliminary estimate of rudder area. It should be noted that such data normally does not take account of different design parameters such as aspect ratio, which in turn influence hydrodynamic efficiency and hence required rudder area.

8. EFFECTIVE ASPECT RATIO

8.1 General

A rudder of infinite aspect ratio (e.g. a foil completely spanning a wind tunnel, or rudder with infinitely large plates or fences top and bottom) has the same flow over all sections perpendicular to its span, and the flow is said to be two-dimensional. For finite aspect ratio flow occurs over the ends from high pressure to low pressure sides, this cross flow increasing with decreasing span, and the flow is said to be three-dimensional. If the root of the rudder is working sufficiently close to a flat surface (say hull) so that there is no cross flow at the root, then the rudder characteristics (e.g. lift and drag) become identical to that of a rudder with twice its geometric aspect ratio; this is best illustrated by the concept of a mirror image, Figure 17, where the geometric aspect ratio of the actual rudder (AR_G) is $S/\bar{c}$ whereas its hydrodynamic performance will be the same as a rudder with an effective aspect ratio (AR_E) of $2 \times S/\bar{c}$.

This complete idealised mirror image effect cannot normally be achieved in practice since there will be a boundary layer present over the adjacent flat plate. This effect is often minimised in the case of wind tunnel tests by the use of a groundboard displaced from the tunnel wall, (see Reference 8). Alternatively the effective geometric span could be reduced by the boundary layer displacement thickness, and the corrected geometric span doubled.

In the case of an actual rudder design the boundary layer and wake effect will normally be accounted for in the assumed design velocity. However, in the case of the movable control surface, such as a rudder, some practical gap at the root of the rudder is required for its operation, the hull adjacent to the rudder will often not be a flat plane, and a rudder on a small craft operating near (or piercing) the water surface will suffer free surface losses; these features lead to a decrease in the ideal mirror image effect, and the Effective Aspect Ratio may be expressed as $AR_E = kAR_G$ where the aspect ratio factor k will be ≤ 2. (For convenience and comparative purposes the free surface effect will also be treated as a loss in effective aspect ratio). For comparative purposes, the relationship between the loss in lift curve slope relative to a decrease in aspect ratio factor k (derived from Equation 2) has been plotted in Figure 18.

The effects of the rudder / hull gap, hull shape and free surface on effective aspect ratio are considered in the next three sections.

8.2 Root Gap Variation

Figure 19 is based on data derived from References 11, 12 and 19, and shows the influence of root gap on effective aspect ratio factor k ($= AR_E/AR_G$).

For example, in going from zero gap (with k = 2) to a gap of $0.005\bar{c}$ k drops to 1.9 (e.g. a rudder with AR_G of 2 has AR_E of 3.8) and decrease in lift curve slope (hence lift) from Equation 2 (or Figure 18) is approximately 2%. This is not much greater than the order of data scatter in deriving Equation 2, hence it can be assumed for design purposes that for gaps up to about $0.005\bar{c}$ (e.g. 2.25mm gap for 450mm chord rudder) AR_E can be assumed 2 x AR_G. 5mm is probably a more realistic minimum gap for a 450mm chord in which case $G/\bar{c} = 0.011$, $k \simeq 1.8$ and decrease in lift curve slope (and lift) is approximately 5%.

It is interesting to observe from Figure 19 that even for root gap ratio of $0.10\bar{c}$ (representing a 45mm gap for 450mm chord rudder) the effective aspect ratio is still about 1.4 x AR_G.

Regarding the influence of gap on $C_{L\ max}$ in respect of strength calculations, the data in References 11 and 12 indicate a relatively insignificant influence on $C_{L\ max}$ for $G/\bar{c}$ values up to about 0.07.

Data relating to the increase in drag for variation in gap size is sparse. However, Figure 20, calculated and estimated from data in References 11 and 12, gives some guidance for the influence on C_{Do} and induced drag factor X. These increases are relatively small. For example, if an increase in C_{Do} of about 0.001 for a $G/\bar{c}$ of 0.01 is related to the drag coefficients in Figure 6b it is seen that the increase can be neglected for most purposes. Similarly, for a $G/\bar{c}$ of 0.01, the increase in induced drag factor X is only about 8%.

Whilst the data indicate that relatively small and acceptable loss in lift curve slope and increase in drag occurs for a root gap of up to say $0.01\bar{c}$, further increase in gap leads to further losses. Although some loss may be acceptable in a workboat or cruising craft in lieu of a more suitable production / assembly design, the data indicate that the gap should be minimised within practical limitations in order to maximise lift / drag ratios for racing or performance craft.

8.3 Shaped Hull above Rudder

Discussion so far has concerned rudders below flat reflection planes; rudders below high speed craft with relatively flat bottoms may well approach this case. However, with hull shape there is a further loss in the

effectiveness of the reflection plane. Figure 21 illustrates the approximate magnitude of this effect. Data from Reference 19 for a rudder with AR_G = 1.5 operating beneath bevelled flat plates showed more rapid fall off in k factor than say data of Reference 10 which was for a simulated submarine hull. Data in Reference 19 is for an immersion of 150mm to top of span of 300mm (i.e. $\bar{h}$ = S/2) which should minimise free surface effects, and Reference 10 does not account for any influence of free surface.

The drag results for the reflection plane and bevelled plate cases in Reference 19 indicated that there was very little difference in C_{Do} due to the bevelled plate (simulating hull shape) but that the bevelled plate case led to an increase in induced drag factor X of about 15% compared with the reflection plane; a reduction in $C_{L\,max}$ of about 10% was observed for the plate bevelled up 15° from the horizontal and about 5% for the plate bevelled up 30°.

The mean curve shown in Figure 21 gives a satisfactory indication of the influence of hull shape on AR_E and it is interesting to note that even as the rudder approaches stall (say 18° - 26° in the small craft field) AR_E is still about 1.7 x AR_G. This data can be used to derive the influence of hull shape on aspect ratio which, in conjunction with Equation 2 can be used to derive the lift curve slope (hence lift) and drag; the influence on rate of rudder response and / or efficiency can then be evaluated.

Consider, for example, a spade (all-movable) rudder with geometric aspect ratio (AR_G) of 2 operating at say 8°. Under a relatively flat hull it may be assumed that its effective aspect ratio (AR_E) is 4.

Hence from Equation 2, $dC_L/d\alpha$ = 0.0627

from Figure 6b @ 8°, (or Equation 5 assuming C_{Do} = 0.01)

C_D = 0.033 and L/D = 15.2

For the shaped hull case :-

from Figure 21, $k = (2 - 0.0132\alpha)$ = 1.89

and $AR_E = 2 \times 1.89$ = 3.78

Hence from Equation 2, $dC_L/d\alpha$ = 0.0611

From Equation 5 (assuming C_{Do} = 0.01, and X = 0.37 x 1.15),

C_D = 0.035 and L/D = 13.97

This simple calculation indicates that, for this particular rudder, the effect of the shaped hull is to reduce the lift curve slope by about 3% and the L/D ratio by about 8%. Using Equation 2 it can be deduced that

the shaped hull has an increasing influence as the design geometric aspect ratio gets smaller.

The data in Reference 19 indicate decreases of 5% to 10% in $C_{L\ max}$ due to hull shape which can be allowed for in strength calculations.

8.4 Influence of Free Water Surface

Rudder Submerged Condition :- A small craft rudder, even whilst in the 'submerged' condition is working relatively near the surface and is likely to suffer free surface losses which are manifested in the production of waves.

Some indication of the influence of surface effects for the submerged rudder is given in References 20 and 21. The work in these Theses, which is mainly theoretical with some experimental backing, is for foils with the relatively large aspect ratio of 4. Reference 22 gives the results for tests on a ship rudder model with aspect ratio 1.68. The data from these references are presented in Figure 22 which shows the influence of depth of immersion (represented by the non-dimensional factor $\bar{h}$ = depth of immersion / span) on aspect ratio factor k and induced drag factor X in Equation 5 (the induced drag in this case being assumed to also include the drag due to wavemaking). It is immediately apparent from these curves that the influence of immersion is very dependent on Froude No. F_s, (in this submerged case based on rudder span). It is seen that as immersion ($\bar{h}$) is decreased, then for small Froude numbers the value of k increases (in the theoretical limit, as $F \to 0$ and $\bar{h} \to 0$, then k approaches 2, i.e. the surface acting as a reflection plane). At a F_s of about 1 the influence of immersion, from theory, would appear to be negligible whilst for higher F_s there is a decrease in k as $\bar{h}$ is reduced. These trends were confirmed by experiments, References 20 and 22, the latter being lower and in agreement with the conclusions of Reference 20 in that the surface effect increases with decrease in aspect ratio. References 20, 21 and 22 all indicate that free surface effects tend to negligible amounts, for all speeds, when the immersion of the top of the rudder is greater than about half the span.

Theory and experiments (Reference 20) indicate a similar trend for the induced drag factor X, Figure 22b, namely for low Froude Numbers the value of X decreases with decreasing immersion $\bar{h}$ whilst at high F_s the value of X increases with decreasing immersion. (NOTE: the theoretical and experimental values of X have been adjusted to give 0.37 at large depth.)

The experiments in Reference 20 also showed the minimum drag coefficient C_{Do} (Figure 22c) at about 0.04 to be considerably higher than the deeply

submerged case (when a value of about 0.01 would have been expected); some of this difference will however be accounted for by the fact that the experiments were carried out at the low Rn of 0.1×10^6.

Rudder Surface Piercing Condition :- Some indication of the influence of surface effects for the surface piercing rudder is given in References 20 and 21. The work in these references is mainly theoretical with some experimental backing for a foil with an aspect ratio of 4. The data from Reference 20 is presented in a simplified manner in Figure 23 which show the influence of Froude Number Fc (based on rudder chord for surface piercing case) on aspect ratio factor k, induced drag factor X (the induced drag in this case being assumed to also include the drag due to wavemaking) and minimum drag coefficient C_{Do}. It is seen from Figure 23a that for very low speeds the water surface forms an effective reflection plane and as $Fc \to 0$, $k \to 2$. However, as speed is increased wavemaking losses are incurred and lift (hence aspect ratio factor k) is reduced. For example, as $Fc \to 1$ the aspect ratio factor k has fallen to about 1, i.e. no surface reflection properties exist and the rudder has an Effective Aspect Ratio the same as its Geometric Aspect Ratio. These data are for the relatively high aspect ratio of 4 but, as discussed in Reference 20, available experimental data indicate that this effect is likely to increase as aspect ratio decreases.

Figures 23b and c based on the experimental data from Reference 20 indicate that, as Fc in increased, appreciable increases in induced drag factor X and minimum drag coefficient C_{Do} are likely.

It is difficult to deduce specific conclusions from the foregoing surface effect data. However, some general conclusions in respect of small craft are immediately apparent.

Firstly, the surface piercing case (e.g. transom rudder) is suitable for low speed (hence small sailing craft) operation. The data does however illustrate the significant surface losses likely to be incurred in the case of the transom rudder as speed is increased; these losses are likely to exceed the effects of the increased lever (from turning centre) enjoyed by this rudder type.

Most sailing craft operate at Fs about 1.2 (Table I) hence for those rudder types which admit flow over the top (per Figure 24(a)) the data would suggest a relatively small change due to 'lack of immersion'; any possible gain suggested by Figure 22a at low Fs is likely to be offset by the lower aspect ratios (i.e. $AR_E < 8$) normally employed in small craft. Further, as the submerged rudder is brought nearer to surface, and if hull effect above

rudder is small, then the submerged rudder becomes effective surface piercing (per Figure 24d) and will therefore incur losses as for the surface piercing case.

The deeply submerged rudder for the sailing craft is likely to suffer surface effects in the inclined condition when the low pressure side may effectively become surface piercing. Adequate hull surface above the rudder would partly overcome this effect.

Attempt should be made on workboats and the like to keep the top of the rudder immersed greater than say half its span, when surface effects will become negligible. Powercraft with reasonable hull width over rudder are unlikely to suffer significant surface effects.

To make more detailed conclusions from the data at this stage would be presumptuous since the flow conditions near the top of small craft rudders mounted well aft, or transom hung, can in any case be confused. It is however considered that the data presented in Figures 22 and 23 should provide useful guidance in assessing the location (longitudinally and vertically) of a new rudder proposal for particular design speed conditions.

9. INFLOW VELOCITY AND ANGLE OF ATTACK

9.1 Estimates have to be carried out or assumptions made for velocity and angle of attack in order to carry out the design calculations.

The free stream condition is likely to be modified by one or several of various influences which may be summarised as follows :

9.2 Inflow Velocity may be modified by :

(a) Wake-retarding influence of hull and deadwood and / or keel ahead.

(b) Propeller - accelerating influence of propeller race for rudders operating in propeller slip stream.

(c) Reduction of speed on a turn.

(d) Orbital velocities of waves.

Attention to item (c) may be paid in the consideration of manoeuvring characteristics, whilst (d) may be considered in respect of coursekeeping, particularly for the case of following seas when craft speed may be similar to wave speed. The basic design condition will, however, normally only consider influences (a) and (b) since these will give an indication of the likely operational Reynolds Number and Froude Number ranges for the rudder, and an estimate of the maximum velocity likely to be encountered in respect of strength calculations. (Poor performance in existing or base design due to influences (c) and (d) would of course require consideration in a new design).

The influence of wake will normally be estimated using empirical data available for small craft, e.g. such as from Reference 23. Typical approximations to the wake fraction are given by :-

$w_T = 0.8\ C_B - 0.26$ for single screw and sailing craft

$w_T = 0.6\ C_B - 0.24$ for twin screw craft

where $w_T = \dfrac{V_s - V_A}{V_s}$

or $V_A = V_s\ (1 - w_T)$

V_A = Advance speed of rudder, corrected for wake.

V_s = Craft Speed.

These formulae are typically suitable for a speed range (based on craft length) of approximately F_n = 0.18 to 0.30; w_T tends to decrease as speed increases and the wake fraction effectively disappears at high speed (e.g. when planing).

Although very little data are available, the trends of the above data are assumed satisfactory for sailing craft; e.g. measurements on a yacht model in way of rudder reported in Reference 24 indicate a wake fraction of about 0.2.

The influence of propeller race will normally be estimated using an empirical correction to the rudder advance speed (corrected for wake).

Typical empirical corrections which can be used are :

From Reference 25	$V_R = 1.15\ V_A$	For low rev/large dia prop up to 500 rpm.
	$V_R = 1.25\ V_A$	For faster, smaller dia. props up to 1500 rpm.
From Reference 3	$V_R = 1.2\ V_S$	For high speed craft.

where V_R = advance speed of rudder, corrected for wake and propeller race.

It is found that the above corrections lead to a velocity past the rudder of about 85% to 95% of P x n (where P = propeller pitch in metres and n = revs/s), the theoretical velocity existing immediately aft of the propeller.

9.3 Inflow angle may be modified by :

(a) Drift angle developed on a turn. This leads to a decrease in the effective angle of attack on the rudder (Figure 25d).

(b) Straightening effect of the hull or deadwood forward of the rudder. This tends to offset the decrease in attack due to drift.

(c) Propeller straightening effect on overall flow tending to offset the effect of drift.

(d) Modification to local rudder angles of attack due to rotation of propeller slipstream.

(e) Leeway in the case of the sailing yacht.

(f) Straightening effect of sailing craft keel (due to downwash) This tends to offset effective increase in angle of attack on rudder due to leeway.

These modifications tend to influence the rudder response rate and

handling characteristics of a craft.

Modification (a) leads to the requirement that the actual helm angle might be somewhat larger than the rudder inflow angle or stall angle. Conversely, modification (e) for a sailing craft with detached rudder implies an angle of attack on rudder with zero helm. However, unless the clear space between a separate keel and rudder is large the downwash effect of the keel (modification (f)) is likely to reduce the leeway effect significantly. A more detailed discussion of these influences on the design and handling of small craft is given in Reference 4.

In respect of structural calculations, the maximum angle of attack is important, the maximum rudder forces at stall normally establishing this design point.

In the case of comparing alternative rudders, or rudder modifications for a particular craft, then arbitrary angles can be safely chosen on the assumption that the modifying factors will not significantly change.

Care has to be exercised in the choice of design rudder angle of attack for a sailing craft at a particular leeway, since it will determine the helm sense carried by the craft, and may also significantly influence the assessment of the performance of a skeg rudder.

10. GENERAL DISCUSSION

10.1 All-Movable Rudders

It will be readily apparent from what has been said that the most important influence on hydrodynamic efficiency is aspect ratio, increase in aspect ratio leading to an increase in efficiency. Whilst the efficiency increases by deepening the rudder, the following observations and possible limitations have to be borne in mind when evolving a satisfactory compromise:-

Possible draught limitation.

A deep rudder is more prone to pick up weeds.

Stall angle decreases appreciably with increasing aspect ratio.

Strength limitations may conflict with hydrodynamic properties due to increased bending moment on the deeper rudder; e.g. in Appendix 4 an example calculation indicates that in increasing the aspect ratio from 3 to 5 for a particular rudder its thickness ratio has to be increased from 0.12 to 0.17 in order to maintain the same strength requirements.

The lowering of rudder centre of pressure with increasing depth (span) leads to adverse heeling moments in the case of the sailing craft.

The data also illustrates the need for the rudder on a sailing craft to operate at or near the maximum lift / drag ratio if drag is to be minimised in the production of a required design side force. An outline calculation in Appendix 5 illustrates how an increase in rudder area may be efficiently employed to meet such requirements on a sailing craft.

Appendix 6 illustrates the use of the all-movable data in the design of a spade rudder for a power craft.

10.2 Skeg Rudders

The data previously discussed have indicated that the skeg rudder will invariably be less hydrodynamically efficient than the all-movable rudder. However this type has become very popular for small (particularly sailing) craft and the following observations are made on its use.

The skeg offers some protection to the movable part of the rudder and offers the possibility of a more robust structural design provided a skeg with adequate rigidity is used, together with a sound lower pintle.

The fixed skeg contributes to directional stability for the 'rudder free' condition, which may be a desirable feature for some sailing craft.

The (skeg / total mean chord) ratio should not exceed about 30% if satisfactory manoeuvring performance is to be achieved. This requirement may of course conflict with the provision of adequate rigidity in the skeg.

The full skeg rudder cannot be balanced, hence leading to relatively high torques, and possible heavy feel for hand held rudders. Using a semi-balanced configuration will help to offset this effect.

10.3 Plate Rudders

The data presented in this report is generally for rudders with a minimum thickness / chord ratio of 0.10. This covers the vast majority of applications in the small craft field, but it is accepted that there are exceptions, when the lifting surface provided by the rudder effectively tends to a flat plate.

The small dinghy is one example where the thickness ratio may be as low as 0.03 - 0.05. Such small thicknesses enjoy a slightly increased lift curve slope and lower minimum drag. However, separation occurs at lower angles of attack than for thicker sections with subsequent increase in drag and decrease in both stall angle and maximum lift. A well rounded, tending to parabolic, nose on such thin rudders will delay the onset of separation.

The principal application of plate rudders is for slow speed craft such as general purpose workboats, where such a rudder welded to rudder stock may be employed. This arrangement is likely to incur higher minimum drag than an aerofoil section but, as concluded in Reference 2, finds satisfactory application for low speed operation and if cost is a factor.

11. CONCLUSIONS AND RECOMMENDATIONS

11.1 A wide range of free-stream rudder data has been presented, together with the relevant corrections to the free stream condition. These data are suitable for small craft rudder design and investigation, where a relatively wide range of variations in design parameters can occur, even for one rudder type. A systematic design approach can be used, either in drawing up comparisons or for deriving absolute rudder forces.

11.2 Aspect ratio has the largest influence on the hydrodynamic characteristics of the rudder. Moderate taper and sweep of the rudder profile have relatively small influences on lift and drag. A normal aerofoil section, such as the N.A.C.A. 00 series provides the best all-round performance for a movable appendage such as the rudder. Available data indicate that if the bottom of the rudder is 'squared off', the hydrodynamic losses (if any) at low angles of attack are small compared with the gains to be made at higher angles of attack.

11.3 The forward-most position of the chordwise centre of pressure moves forward with decreasing aspect ratio, and can be considerably further forward than the 25% $\bar{c}$ normally associated with high aspect ratio foils. Care has therefore to be taken in locating the stock position in order to avoid negative torques and to strike a satisfactory compromise between balance and 'feel' of the helm.

11.4 Whilst the rate of increase of lift for the skeg-rudder combination can be considerably less than the all-movable equivalent, its stall angle is delayed and the maximum lift achieved is about the same. Drag is however higher and hence lift / drag ratios are lower than for the all-movable rudder.

11.5 An improvement in skeg-rudder characteristics follows if gap size between rudder and skeg is minimised. However, even with the gap sealed the skeg rudder falls short of the rate of increase in lift attainable by the all-movable rudder.

11.6 Negative angles of attack on the skeg of the skeg-rudder are likely and lead to reduced performance when manoeuvring, with much lower rate of response than the all-movable rudder and the added penalty of higher drag.

11.7 Skeg chord length should not exceed about 30% of the total skeg-rudder mean chord if satisfactory all-round performance is to be provided. This may however conflict with the provision of adequate structural rigidity in the skeg.

11.8 Hull-rudder root gap and shaped hull above the rudder both contribute to a loss in rate of increase in sideforce, and increase in drag, with increase in rudder angle of attack. Whilst some loss due to gap may be acceptable for a workboat or cruising craft in lieu of a more suitable production / assembly design, hull-rudder gap should be minimised within practical limitations in order to maximise lift / drag ratios for racing or performance craft.

11.9 Free surface effects can have a significant influence on rudder performance, these effects increasing with craft speed.

For the 'submerged' rudder, free surface effects tend to be negligible for all speeds when the immersion to the top of the rudder is greater than about half its span.

For the transom hung ("surface piercing") rudder, free surface losses are highly speed dependent, and the data indicate that such rudders are only hydrodynamically suitable for low speed use.

REFERENCES

1. Abbot I.H. and Von Doenhoff A.E. : "Theory of Wing Sections". Dover Publications, New York 1958.

2. Gregory D.L. and Dobay G.F. : "The Performance of High-Speed Rudders in a Cavitating Environment". Trans. SNAME, 1973.

3. Du Cane P. : "High Speed Craft" Temple Press.

4. Marchaj C.A. : "Sailing Theory and Practice". Adlard Coles, 1964.

5. Millward A. : "The Design of Spade Rudders For Yachts". Southampton University Yacht Research Report No. 28, 1969.

6. Jones G.W. Jr. : "Aerodynamic Characteristics of Three Low Aspect Ratio Symmetrical Wings with Rectangular Planforms at Reynolds Numbers between 0.4×10^6 and 3.0×10^6". NACA RM L52G18, 1952.

7. Jacobs E.N. and Anderson R.E. : "Large Scale Characteristics of Airfoils as Tested in the Variable Density Wind Tunnel". NACA Report No. 352, 1930.

8. Whicker L.F. and Fehlner L.F. : "Free Stream Characteristics of a Family of Low Aspect Ratio Control Surfaces for Application to Ship Design". D.T.M.B. Report 933, December 1958.

9. Comstock J.P. (Ed) : "Principles of Naval Architecture". SNAME, New York 1967.

10. Harper J.J. and Simitses G.J. : "Effect of a Simulated Submarine Hull on the Characteristics of All-Movable Control Surfaces". Georgia Institute of Technology, Report 439 August 1959.

11. Kerwin J.E., Mandel P. and Lewis S.D. : "An Experimental Study of a Series of Flapped Rudders". Journal of Ship Research, SNAME, December 1972.

12. Molland A.F. : "The Free Stream Characteristics of a Semi-Balanced Ship Skeg-Rudder". University of Southampton, Ship Science Report No. 3/77 (Includes reference to extension of experiments described in this Report).

13. Hoerner S.F. : "Fluid Dynamic Drag". Publ. by Author, 1965

14. Ames M.B. Jr. and Sears R.I. : "Pressure-Distribution Investigation of an N.A.C.A. 0009 Airfoil with a 30-Percent-Chord Plain Flap and Three Tabs". N.A.C.A., TN No 759, 1940.

15. Street W.G. and Ames M.B. Jr. : "Pressure-Distribution Investigation of an N.A.C.A. 0009 Airfoil with a 50-Percent-Chord Plain Flap and Three Tabs". N.A.C.A TN No 734, 1939.

16. Ames M.B. Jr. and Sears R.I. : "Pressure-Distribution Investigation of an N.A.C.A. 0009 Airfoil with an 80-Percent-Chord Plain Flap and Three Tabs". N.A.C.A. TN No 761, 1940.

17. Jaeger H.E. : "Approximate Calculation of Rudder Torque and Rudder Pressures". International Shipbuilding Progress, Vol. No. 10, 1955.

18. Myers H.A. : "Theory of Sailing Applied to Ocean Racing Yachts". Marine Technology, S.N.A.M.E., Vol. 12. No.3, 1975.

19. Molland A.F. : "Free Stream Test Tank Data for a Spade Rudder - 1975 (Unpublished).

20. Millward A. : "The Induced Drag of a Vertical Hydrofoil". Ph.D. Thesis, University of Southampton, Department of Aeronautics and Astronautics, 1967.

21. Ismail K.A.R. : "The Hydrodynamic Theory of Vertical Swept Hydrofoils near a Free Surface and Comparison with Measurement". Ph.D. Thesis, University of Southampton, Department of Aeronautics and Astronautics, 1973.

22. Shiba H. : "Model Experiments about the Manoeuvrability and Turning of Ships". First Symposium on Ship Manoeuvrability, D.T.M.B. Report 1461, October 1960.

23. Barnaby K. : Basic Naval Architecture, Hutchinson.

24. Spens P.G., De Saix P. and Brown P.W. : "Some Further Experimental Studies of the Sailing Yacht". Trans. S.N.A.M.E. Vol. 75, 1967.

25. Hatch G.N. : "Creative Naval Architecture". Reed Publishing, 1971.

26. Performance Prediction of Small Craft : R.I.N.A. Occasional Publication No. 1, 1974.

27. Taplin A. : "Notes on Rudder Design Practice". First Symposium on Ship Manoeuvrability, D.T.M.B. Report 1461, October 1960.

	Length WL (m)	Assumed Speed V knots	Assumed Speed V m/s	RUDDER: Assumed Rudder Chord $\bar{c}$ (m)	RUDDER: $R_n = \frac{V\bar{c}}{\nu}$ $\nu = 1.19 \times 10^{-6}$	RUDDER: $F_c = \frac{V}{\sqrt{g.\bar{c}}}$	RUDDER: F_s $(AR_G=2)$ $= \frac{V}{\sqrt{g.S}}$
	4.5	2.5	1.29	0.2	0.22×10^6	0.92	.65
Sailing	4.5	5.4	2.78	0.2	0.47×10^6	1.98	1.40
	6	6.2	3.19	0.4	1.07×10^6	1.61	1.14
Craft	9	7.6	3.91	0.6	1.97×10^6	1.61	1.14
	12	8.8	4.53	0.7	2.66×10^6	1.73	1.22
Power	15	10	5.15	0.4	1.73×10^6	2.60	1.83
Craft	25	40	20.6	0.5	8.65×10^6	9.30	6.58
	30	10	5.15	1.0	4.32×10^6	1.64	1.16

Table 1 Typical Reynolds and Froude Numbers (based on rudder chord) for Small Craft.

APPENDIX 1

DESIGN FORMULAE

ALL-MOVABLE RUDDERS :-

$$C_L = \left(\frac{dC_L}{d\alpha}\right)_{\alpha=0} \times \alpha + \frac{C_{D_c}}{AR_E} \left(\frac{\alpha}{57.3}\right)^2 \quad \text{. . . . . 1}$$

where $$\left(\frac{dC_L}{d\alpha}\right)_{\alpha=0} = \frac{2\pi}{57.3\ (1 + 3/AR_E)} \quad \text{. . . . . 2}$$

and $$C_{D_c} = 0.1 + 1.6\ C_T/C_R \text{ -- Square Tips . . . . . 3}$$

$$= 0.1 + 0.7\ C_T/C_R \text{ -- Faired Tips . . . . . 4}$$

$$C_D = C_{D_o} + X.\frac{C_L^2}{AR_E} \quad \text{. . . . . 5}$$

where X = 0.37 may be assumed as a satisfactory value for practical design purposes.

$$C_N = C_L.\cos\alpha + C_D.\sin\alpha \quad \text{. . . . . 6}$$

$$C_R = \sqrt{C_L^2 + C_D^2} \quad \text{. . . . . 7}$$

Centre of pressure - chordwise - from leading edge :

$$CP\bar{c} = \left(0.25 - \frac{C_m' \bar{c}/4}{C_N}\right) . \bar{c} \quad \text{. . . . . 8}$$

where $$C_{m\,\bar{c}/4}' = \left[0.25 - \left(\frac{dC_m'}{dC_L}\right)_{C_L=0}\right].\left(\frac{dC_L}{d\alpha}\right)_{\alpha=0} \times \alpha - \frac{1}{2}.\frac{C_{D_c}}{AR_E}.\left(\frac{\alpha}{57.3}\right)^2 \text{ --9}$$

and $$\left(\frac{dC_m'}{dC_L}\right)_{C_L=0} = \frac{0.25}{(1 + 1/AR_E)} \quad \text{. . . . . 10}$$

Centre of Pressure, spanwise, from root :

$$CP_S = \left[\frac{0.85}{(5 + AR_E)} 0.25 \times \left(\frac{C_T}{C_R}\right)^{0.11}\right].S \quad \text{. . . . . 11}$$

(valid for AR_E range 1 to 6 and Taper Ratio range 0.6 to 1.0

Formulae, 1 to 11 provide a satisfactory fit to available data for design purposes for thickness / chord (t/c) range 0.10 to 0.15. (A small increase in lift curve slope follows for t/c < 0.10 and a small decrease in lift curve slope follows for t/c > 0.15)

SKEG RUDDERS:-

$$\text{Skeg rudder lift / Equiv. all movable} = \frac{L_S}{L} = \frac{2.4}{\left(1.4 + \frac{1}{A_m/A_T}\right)} \quad \text{-- 12}$$

$$\text{Lift of movable part } L_m = \frac{C_m}{2C_S + C_m} \times L_T \quad \text{- - - - - - - - 13}$$

RUDDER STOCK SIZE:-

Torque on rudder stock

$$T = N \times \bar{x} \quad \text{- 14}$$

Bending moment about rudder root

$$M = R \times CPs \times S \quad \text{- 15}$$

Equivalent Bending Moment

$$BM_E = \frac{M}{2} + \frac{1}{2}\sqrt{M^2 + T^2} \quad \text{- - - - - - - - - - - - - - - - 16}$$

Equivalent Torque

$$T_E = M + \sqrt{M^2 + T^2} \quad \text{- - - - - - - - - - - - - - - - - - - 17}$$

Diameter of solid stock

$$d = \sqrt[3]{\frac{BM_E \times 32}{\pi \times \sigma}} \quad \text{or} \quad = \sqrt[3]{\frac{T_E \times 16}{\pi \times \sigma}} \quad \text{- - - - - - - - - - 18}$$

where say σ = 50% of yield strength of rudder stock material. For an assumed value of σ, (from 18) :-

$$d \propto \sqrt[3]{T_E} \quad \text{- 19}$$

$$\text{or} \quad d \propto \sqrt[3]{BM_E} \quad \text{- 20}$$

For equivalent tubular rudder stock outside and inside diameters d_1 and d_2 have to satisfy following equation :-

$$d = \sqrt[3]{\frac{d_1^4 - d_2^4}{d_1}} \quad \text{- - - - - - - - - - - - - 21}$$

APPENDIX 2

COMPARISONS BETWEEN SKEG AND ALL-MOVABLE RUDDERS

Assume a lift coefficient of 0.33 is required, based on the same total rudder areas.

Using Figure 11, (AR_E = 2.8) for C_m/c = 60%

	All-movable	Skeg rudder
C_L	0.33	0.33
Required α	7^o	9.8^o
L/D	11.0	6.8
C_D	0.030	0.049

i.e. an approximate increase in $C_D = \frac{0.049 - 0.030}{0.030} = 60\%$

For a rudder of span 0.8m, chord 0.4m at a speed of 2.5 m/s this amounts to a total original drag on the all-movable rudder of :-

$$D = 0.030 \times \frac{1025}{2} \times 0.32 \times 2.5^2 = 30.75N$$

and an increase in drag when using a comparable skeg rudder of approx:-

$$D = (0.049 - 0.030) \times \frac{1025}{2} \times 0.32 \times 2.5^2 = 19.48N$$

If the calculations are repeated with an assumed leeway at rudder of 5^o, i.e. from Figure 25b this requires a weather helm on the all-movable rudder of 2^o for effective α of 7^o.

From Figure 9c @ $\beta = +5^o$

$C_L = 0.33$ achieved at $\delta = 4.5^o$

and $C_D = 0.045$, hence L/D = 7.33

This amounts to an approximate increase in C_D of 50%

APPENDIX 3

DERIVATION OF APPROXIMATE MAXIMUM TORQUE ON SKEG RUDDER STOCK.

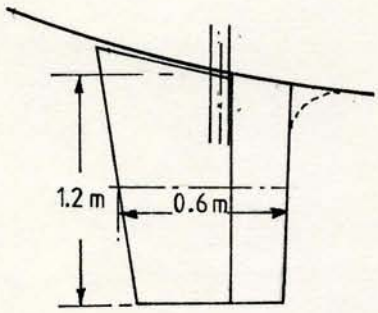

Assume skeg rudder with mean chord

$\bar{c}$ = 0.6m

span S = 1.2m

hence AR_G = 2

Assuming rudder closely fitted to hull,

AR_E = 4

Assume skeg chord= 30% of total

and speed= 7 knots = 3.61 m/s

From Figure 13, for $Am/A_T = 0.7$, $Ls/L \doteq 0.84$; this similarly follows by comparing Figure 10 with Figure 6a, i.e. lift on rudder plus skeg combination is 84% of all-movable equivalent for most of lift curve; $C_L max$ for skeg rudder will however be about the same as all-movable. Hence from all-movable data, Figure 6a, assuming $C_L max$ at $\beta = 0$ is same as for all-movable (although α_{stall} will be larger), for $AR_E = 4$, $C_L max = 1.01$ for all-movable equivalent. Maximum lift (rudder + skeg)

$$= C_L max \times \tfrac{1}{2}\rho A V_R^2$$

$$= 1.01 \times \frac{1025}{2} \times 0.72 \times 3.61^2$$

$$= 4856.9 \text{ N}$$

From Figure 14, for $C_m/c = 0.7$, lift on MOVABLE part of rudder

$$\doteq 54\% \text{ of total}$$

$$= 0.54 \times 4856.9 = 2622.7 \text{ N}$$

and acts approx 0.4 Cm aft of stock at stall.

i.e. 0.4 x (0.7 x 0.6) = 0.168 m aft stock.

In absence of drag data, maximum normal force is assumed equivalent to the maximum lift for torque calculations.

Hence torque on stock = 2622.7 x 0.168

= 440.6 Nm

From equation 17, Equivalent torque $T_E = T = 440.6$ Nm

Assuming a design stress of 130 N/mm^2 for m.s., i.e. about half yield strength

$$\text{Stock diameter } d = \sqrt[3]{\frac{T_E \times 16}{\pi \times \sigma}} = \sqrt[3]{\frac{440.6 \times 16}{\pi \times 130 \times 1000^2}} \times 1000$$

$$= 24.8 \text{ mm}$$

This assumes all bending is carried by skeg. If say 30% of bending moment is assumed to be carried by skeg, then moment carried by stock is

$$M = 4856.9 \times 0.70 \times (1.2 \times 0.48)^{CPs}$$

$$= 1958.3 \text{ Nm.}$$

$$\text{and } BM_E = \frac{1958.3}{2} + \tfrac{1}{2} \sqrt{1958.3^2 + 440.6^2}$$

$$= 1982.8 \text{ Nm}$$

$$\text{and stock diameter } d = \sqrt[3]{\frac{1982.8 \times 32}{\pi \times 130 \times 1000^2}} \times 1000$$

$$= 53.8 \text{ mm}$$

plus say 2 x 10 mm for rudder structure abreast stock

gives $t_{max} = 73.8$

and $t/c = \frac{78.8}{600} = 0.123 = 0.12$

Using the properties of the skeg material and construction, a check on the skeg root bending moment and hence stresses would be required to confirm that this thickness is satisfactory.

APPENDIX 4

RELATIONSHIP BETWEEN ASPECT RATIO AND THICKNESS RATIO TO MEET STRUCTURAL REQUIREMENTS

Assume a spade rudder fitted close to hull of a sailing yacht has an area of 0.40 m^2, an effective aspect ratio of 3 and a thickness ratio (t/c) of 0.12.

It is proposed to fit a new rudder with an effective aspect ratio of 5, and an area necessary to develop the same lift as the original rudder in an assumed design condition of 6^o effective angle of attack and a speed of 6 knots. It is required to determine the area of the new proposal and the decrease in rudder drag, for the design conditions, and the root bending moments at stall for the original and new proposals.

ORIGINAL RUDDER	NEW PROPOSAL
$AR_E = 3$	$AR_E = 5$
Speed $V_R = 6 \times 0.515 = 3.09$ m/s	$V_R = 3.09$ m/s
at 6^o, from Fig. 6a, $C_{L_o} = 0.330$	$C_{L_N} = 0.414$
	since $C_L = \frac{L}{\frac{1}{2}\rho A V_R^2}$
	$A \propto 1/C_L$
Therefore for same lift,	
	New area $A_N = A_o \times \frac{C_{L_o}}{C_{L_N}}$
	$= 0.40 \times \frac{0.330}{0.414}$
	$= \underline{0.319\ m^2}$
$\bar{c} = \sqrt{\frac{\text{Area}}{AR_G}} = \sqrt{\frac{0.40}{1.5}}$	$\bar{c} = \sqrt{\frac{0.319}{2.5}}$
$= 0.516$ m	$= 0.357$ m.
and $S = \frac{0.40}{0.516} = 0.775$ m	$S = \frac{0.319}{0.357} = 0.894$ m
$R_n = \frac{V\bar{c}}{\nu} = \frac{3.09 \times 0.516 \times 10^6}{1.19}$	$R_n = \frac{3.09 \times 0.357 \times 10^6}{1.19}$
$= 1.34 \times 10^6$	$= 0.927 \times 10^6$

From Figs. 6e and 6b, or Eqn 5 for thickness ratio t/c = 0.12 :-

$C_{D_o} = 0.011$ $C_{D_o} = 0.0115$

@6° $C_D = 0.024$ $C_D = 0.024$

Drag $D = C_D \times \frac{1}{2}\rho A V_R^2$

$= 0.024 \times \frac{1025}{2} \times 0.4 \times 3.09^2$ $D = 0.024 \times \frac{1025}{2} \times 0.319 \times 3.09^2$

$= 46.98$ N. $= 37.46$ N.

Hence Decrease in drag = 9.52 N, i.e. about 20% of original

From Figs 6c, d and b.

$\alpha_{stall} = 22^\circ$, $C_L max = 0.90$ $\alpha_{stall} = 18.2^\circ$, $C_L max = 0.935$

$C_D = 0.208$ $C_D = 0.128$

$C_N = C_L \cos\alpha + C_D \sin\alpha$

$= 0.90 \times 0.927 + 0.208 \times 0.375$ $C_N = 0.935 \times 0.950 + 0.128 \times 0.31$

$= 0.912$ $= 0.928$

$N = C_N \times \frac{1}{2}\rho A V_R^2$

$= 0.912 \times \frac{1025}{2} \times 0.4 \times 3.09^2$ $N = 0.928 \times \frac{1025}{2} \times 0.319 \times 3.09^2$

$= 1785.1$ N $= 1448.6$ N.

Assuming stock is situated 7% $\bar{c}$ ford of $CP\bar{c}$ at stall in both cases

lever, $\bar{x} = 0.07 \times 0.516 = 0.036$ m $\bar{x} = 0.07 \times 0.357 = 0.025$ m

and Torque $T = N \times \bar{x}$

$= 1785.1 \times 0.036$ $T = 1448.6 \times 0.025$

$= 64.3$ Nm $= 36.2$ Nm

Resultant Force $R = \sqrt{C_L^2 + C_D^2} \times \frac{1}{2}\rho A V_R^2$

$= \sqrt{.90^2 + .208^2} \times \frac{1025}{2} \times 0.4 \times 3.09^2$ $R = \sqrt{.935^2 + .128^2} \times \frac{1025}{2} \times$

$= 1808.1$ N $0.319 \times 3.09^2 = 1473.1$

From Fig. 6g at stall CPs = 49.2%S

i.e. $CPs = 0.492 \times 0.775 = 0.381$ $CPs = 0.467 \times 0.894 = 0.417$ m

$M = R \times CPs$

$= 1808.1 \times 0.381 = 688.9$ Nm $M = 1473.1 \times 0.417 = 614.3$ Nm

Equivalent bending moment:-

$$BM_E = \frac{M}{2} + \frac{1}{2}\sqrt{M^2 + T^2}$$

$$\therefore BM_E = \frac{688.9}{2} + \tfrac{1}{2}\sqrt{688.9^2 + 64.3^2} \qquad BM_E = \frac{614.3}{2} + \tfrac{1}{2}\sqrt{614.3^2 + 36.2^2}$$

$$= 690.4 \text{ Nm} \qquad = 614.8 \text{ Nm}$$

From Equation 20

$$\text{Stock Diameter} \quad d \propto \sqrt[3]{BM_E}$$

Original rudder has thickness ratio t/c = 0.12
c = 0.516, $\therefore$ t = 62 mm
and stock diameter of say 40 mm

For new proposal, required thickness =

$$40 \times \sqrt[3]{\frac{614.8}{690.4}} + (62-40)$$

t = 60.5 mm

and chord = 0.357 m = 357 mm
hence t/c = 0.17.

From Figure 6e, this thickness ratio increase leads to an increase in C_{D_o} for the new design of about 0.001 which, together with the smaller area of the new design, leads to a net decrease in minimum drag (as $\alpha \to 0$) of about 9% compared with a decrease of about 17% if t/c had remained at 0.12; similarly the 25% increase in L/D ratio at 6^o if t/c remained constant at 0.12 is reduced to a 20% increase when the increase in t/c to 0.17 is allowed for.

APPENDIX 5

INFLUENCE OF LIFT / DRAG RATIO :-

To illustrate possible beneficial effects of increase in rudder area for a sail craft rudder; consider the rudder design for a One-Tonner :-

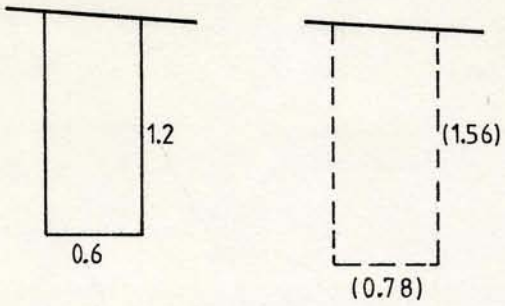

Assume existing design with $AR_G = 2$ (Assumed $AR_E = 4$) with chord 0.6 m span 1.2 m (hence area 0.72 m^2) is required to operate at 10^o attack in order to produce the desired sideforce at say 6 knots (3.09 m/s)

From Figure 6a, at $\alpha = 10^o$ for $AR_E = 4$, $C_L = 0.638$ and $\frac{L}{D} = 13.6$
Assuming AR remains unchanged, angle of attack for max. L/D is 6^o, when L/D = 17; at $\alpha = 6^o$, $C_L = 0.38$.

$$C_L = \frac{L}{\frac{1}{2}\rho A V_R^2}$$

Hence for same lift, $A \propto \frac{1}{C_L}$

and new Area = 0.72 x 0.638/0.38 = 0.72 x 1.679 = 1.21 m^2

(hence new $\bar{c} = \sqrt{\frac{\text{Area}}{AR_G}} = \sqrt{\frac{1.21}{2}} = 0.777$ m

and new S = 1.21/0.777 = 1.56 m

For original area, At 10^o, $C_D = 0.045$, and $D = C_D \times \frac{1}{2}\rho A V_R^2$
$= 0.045 \times \frac{1025}{2} \times 0.72 \times 3.09^2$
$= 158.6$ N

For new area, At 6^o, $C_D = 0.022$ and $D = 0.022 \times \frac{1025}{2} \times 1.21 \times 3.09^2$
$= 130.3$ N

i.e. a saving in drag of 28.3 N i.e. approx. 18%

The minimum drag coefficient (as $\alpha \to 0$) for both rudders is approximately the same at 0.01 and increase in drag for the new design will be proportional to the increase in area.

i.e. for original design, drag $D = 0.01 \times \frac{1025}{2} \times 0.72 \times 3.09^2$
$= 35.2$ N

for new design $D = 0.01 \times \frac{1025}{2} \times 1.21 \times 3.09^2$

$= 59.2$ N

i.e. an increase of 24 N i.e. approx. 68%

These simple calculations for a particular case indicate that an increase in rudder area of about 68% with subsequent decrease in angle of attack has led to a decrease in drag of 28.3 N (about 18%) whilst producing the same sideforce. This saving in drag of 28.3 N for the production of a chosen sideforce is made at the cost of an increase in drag of 24 N at zero angle of attack. It can be deduced from the data that upward of about $4\frac{1}{2}^{o}$ the larger rudder incurs less drag than the smaller rudder for the production of equal sideforce.

Such an increase in rudder area is of course only of benefit when, in order to generate a particular sideforce, the original design has to work at an angle of attack somewhat larger than that for L/D max.

APPENDIX 6

APPLICATION OF DATA TO SIMPLE DESIGN PROCESS

Forces and stock size are required for a spade rudder acting in the slipstream of a relatively low rev. prop. on a semi-displacement craft of length 14 m, $C_B = 0.55$ and maximum speed 18 knots (9.27 m/s). The hull is assumed to be moderately shaped in way of rudder, and the gap between rudder and hull to be 10 mm.

Geometric Aspect Ratio, $AR_G = 1.5$ and Taper Ratio = 0.80 are satisfactory compromises for this vessel type.

From Figure 16, required Area $A = 0.34\ m^2$

$$\text{Hence } \bar{c} = \sqrt{\frac{A}{AR_G}} = \sqrt{\frac{0.34}{1.5}} = 0.476 \text{ m}$$

$$\text{and span } S = 0.34 / 0.476 = 0.714 \text{ m}$$

From Section 9.2, approximate wake fraction = $0.8\ C_B - .26 = 0.18$
and assume correction due to propeller slipstream is $V_R = 1.15\ V_A$
Hence rudder inflow speed, corrected for wake and propeller effects is

$$V_R = 9.27\ (1 - 0.18) \times 1.15$$

$$= 8.74 \text{ m/s.}$$

$$\text{Reynolds No. } Rn = \frac{V\bar{c}}{\nu} = \frac{8.74 \times 0.476}{1.19} \times 10^6$$

$$= 3.5 \times 10^6$$

Assume in first instance that t/c = 0.15 (i.e. max thickness = 71.4 mm) and $AR_E = 2 \times AR_G = 2 \times 1.5 = 3$. Hence from Figure 6c α_{stall}, for t/c = 0.15, $\alpha_{stall} = 26^o$.

From Figure 6d, $C_L max = 1.32$
Figure 6b, $C_D = 0.290$

Gap G = 10 mm

$\therefore$ G/c = 10/476 = 0.021

Hence (from SECTION 8.2) there is no significant influence on $C_L max$ due to gap.

From Figure 20, due to gap, increase in $C_{D_o} = 0.0016 \doteqdot 0.002$

From Figure 6e, $C_{D_o} \doteqdot 0.010$ for no gap, hence corrected C_{D_o} with gap = 0.012

From Figure 20, induced drag factor X = 0.45

from Equation 5, $C_D = C_{D_o} + X \times \frac{C_L^2}{AR_E}$

Hence drag from Figure 6b corrected as follows :-

Corrected $C_D = 0.012 + (0.290 - 0.01) \times \frac{0.45}{0.37}$

for Hull Shape (SECTION 8.3) 10% reduction in $C_L$max, and 15% increase in X and C_{D_o} unchanged.

Hence corrected $C_L = 1.32 \times 0.9 = 1.188$

and corrected drag $= 0.012 + (0.290 - 0.01) \times \frac{0.45}{0.37} \times 1.15 \times \frac{1.188^2}{1.32^2}$

i.e. $C_D = 0.329$

Hence at stall, $C_N = C_L \cos\alpha + C_D \sin\alpha$

$= 1.188 \cos 26 + 0.329 \sin 26$

$= 1.21$

and normal force $N = C_N \times \frac{1}{2}\rho A V_R^2$

$= 1.21 \times \frac{1025}{2} \times 0.34 \times 8.74^2$

$= 16{,}105.8$ N

Resultant force $R = \sqrt{C_L^2 + C_D^2} \times \frac{1}{2}\rho A V_R^2$

$= \sqrt{1.188^2 + 0.329^2} \times \frac{1025}{2} \times 0.34 \times 8.74^2$

$= 16{,}408.1$ N

From Figure 6f, forwardmost position of CP_c = 19% aft LE hence locate stock at say 14% aft LE.

CP_c at stall = 23.5% aft LE

hence lever $\bar{x} = \frac{(23.5 - 14)}{100} \times 0.476 = 0.045$ m

From Figure 6g, CPs at stall = 49.2% S from root

$= 0.492 \times 0.714$

$= 0.351$ m

plus say 20 mm from top of rudder to bearing gives total bending moment lever = 0.351 + 0.02 = 0.371 m.

Hence at stall, torque $T = N \times \bar{x}$

$= 16105.8 \times 0.045$

$= 724.8$ Nm

Bending Moment $M = R \times CPs \times S$

$= 16408.1 \times 0.371$

$= 6087.4$ Nm

Equivalent bending moment $BM_E = \frac{6087.4}{2} + \frac{1}{2}\sqrt{6087.4^2 + 724.8^2}$

$= 6108.9$ Nm

and stock diameter $d = \sqrt[3]{\frac{6108.9 \times 32}{\pi \times 130 \times 1000^2}} \times 1000$

(assuming a design stress of 130 N/mm^2 for M.S., i.e. about half yield strength.)

i.e. $d = 78.2$ mm

Allowing say 5 mm for plating each side of stock, overall rudder thickness would amount to 88.2 mm; this leads to a thickness ratio t/c of 0.19. This would lead to a decrease in $C_L$max to a new value of approx. 1.24 (Figure 6d).

Further iteration could be carried out, leading to a small decrease in stock size.

NOTE:- If the above calculation is repeated with speed correction included, but neglecting the influence of gap and hull shape, the stock diameter derived is 80.6 mm, and hence design stress about 119 N/mm^2. This illustrates that whilst corrections for gap and hull shape give useful indications of their influence on lift curve slope and rudder response over the working range, their inclusion is not critical for the derivation of stock size.

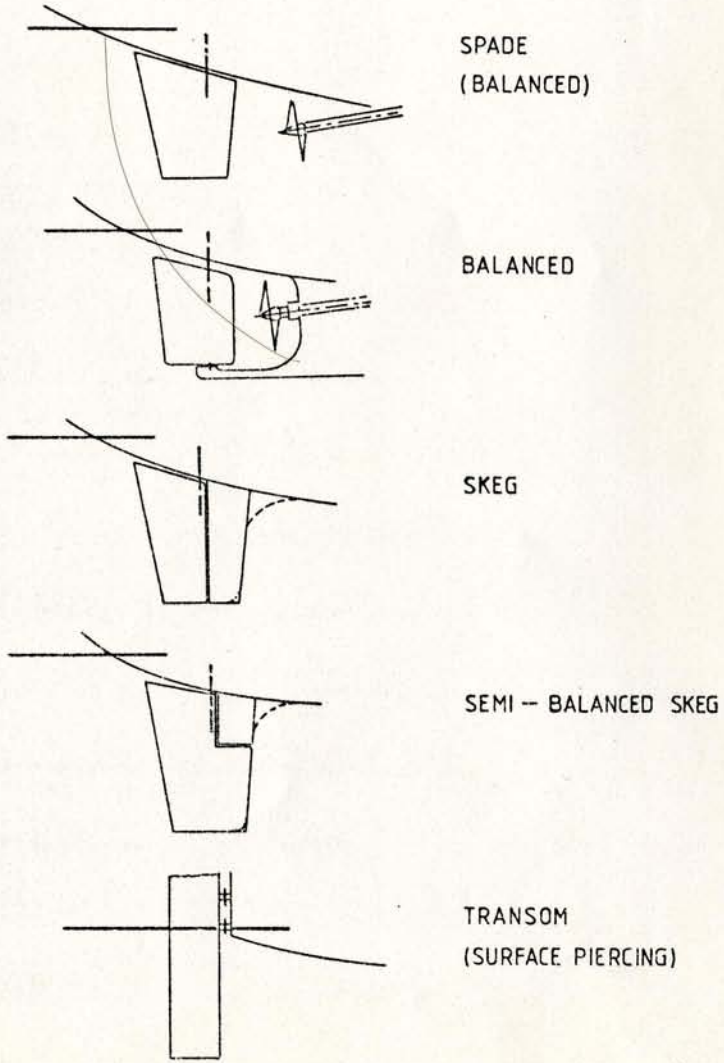

Fig.1 PRINCIPAL SMALL CRAFT RUDDER TYPES

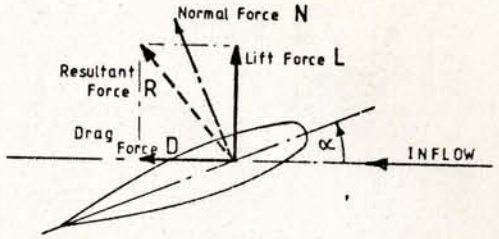

Fig. 2 FORCES ACTING ON RUDDER : (ALL-MOVABLE)

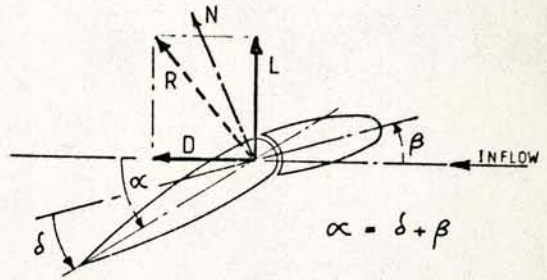

Fig. 3 FORCES ACTING ON RUDDER : (SKEG TYPE)

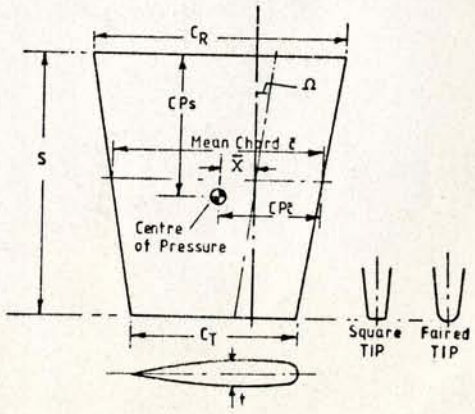

Fig. 4 NOTATION

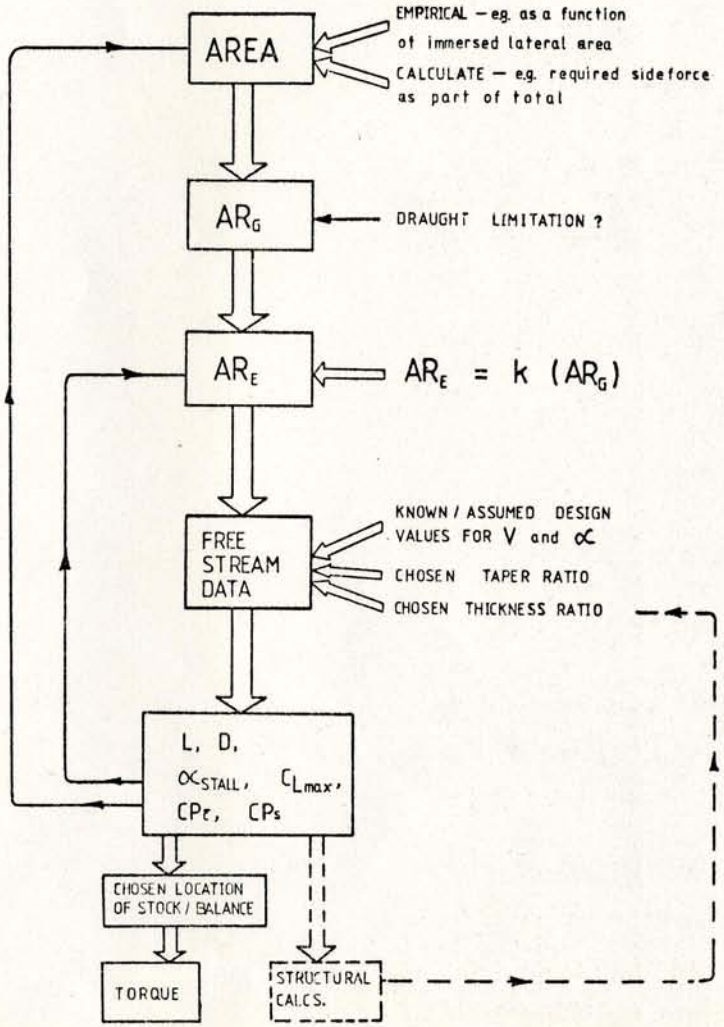

Fig. 5 TYPICAL RUDDER DESIGN PATH

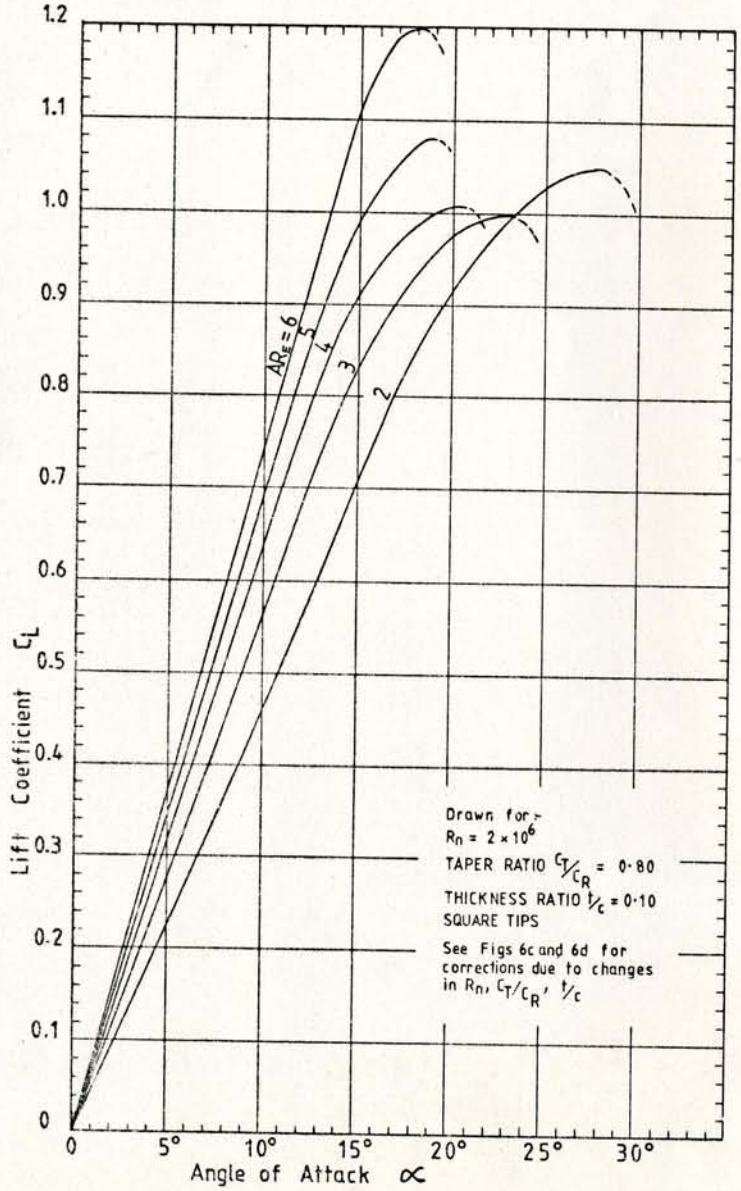

Fig. 6a LIFT COEFFICIENT : ALL-MOVABLE RUDDERS

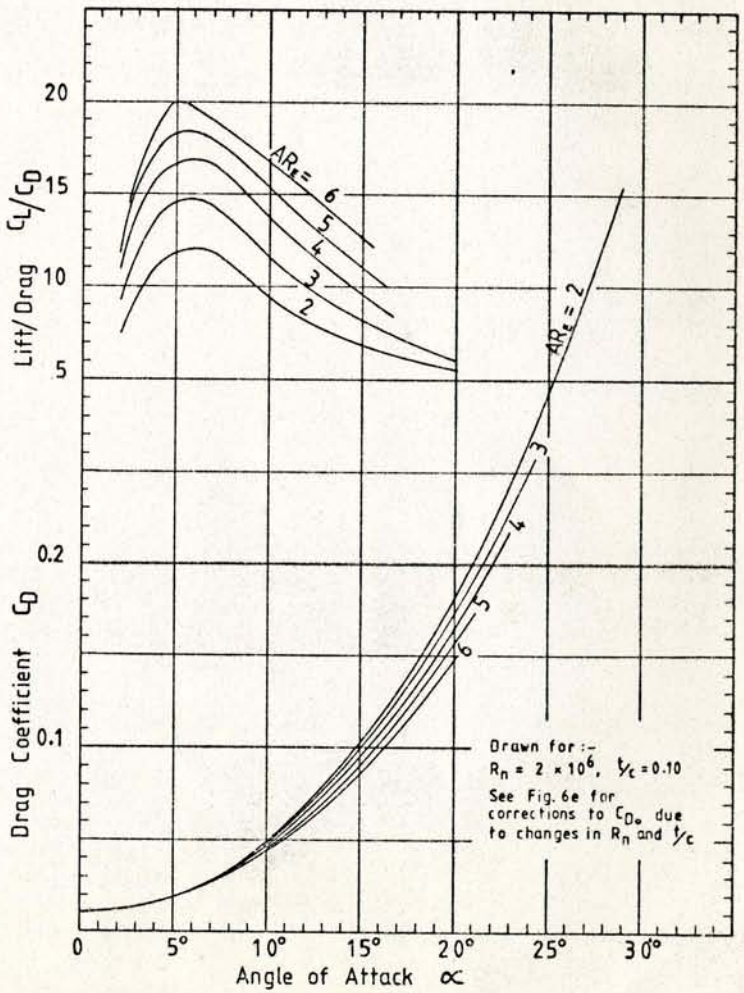

Fig. 6b DRAG COEFFICIENT and LIFT / DRAG RATIO ALL-MOVABLE RUDDERS

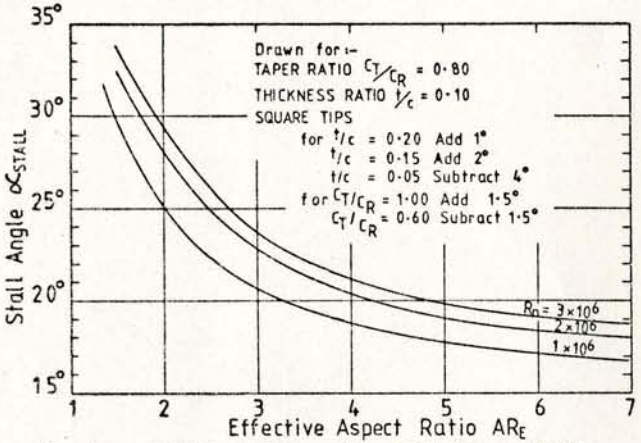

Fig. 6c STALL ANGLE : ALL-MOVABLE RUDDERS

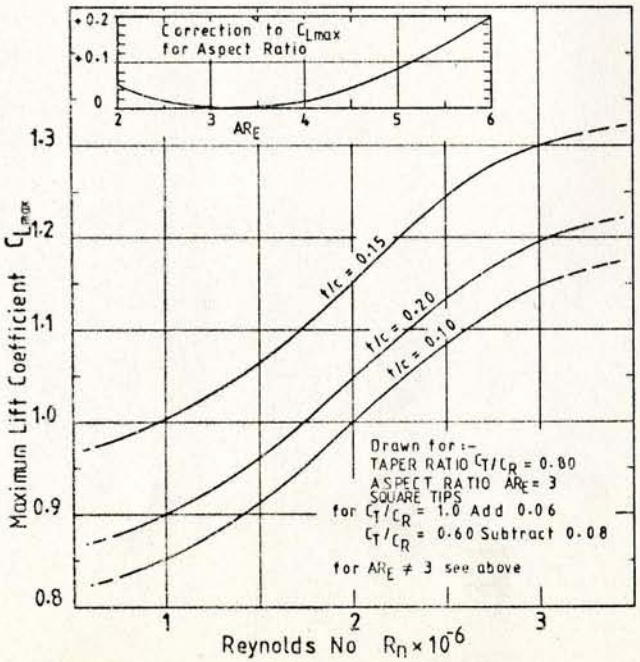

Fig. 6d MAXIMUM LIFT COFFICIENT :

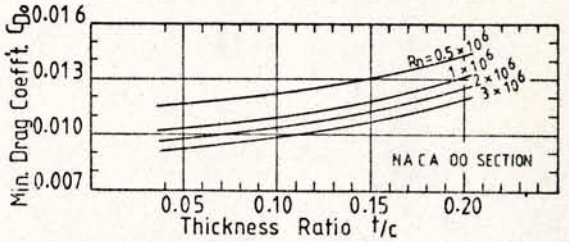

Fig. 6e MINIMUM DRAG COEFFICIENT : ALL-MOVABLE RUDDERS

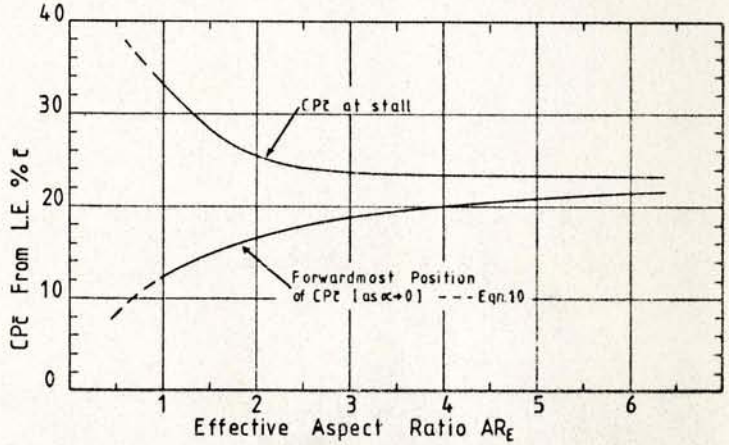

Fig. 6f CENTRE OF PRESSURE (CHORDWISE):
ALL-MOVABLE RUDDERS

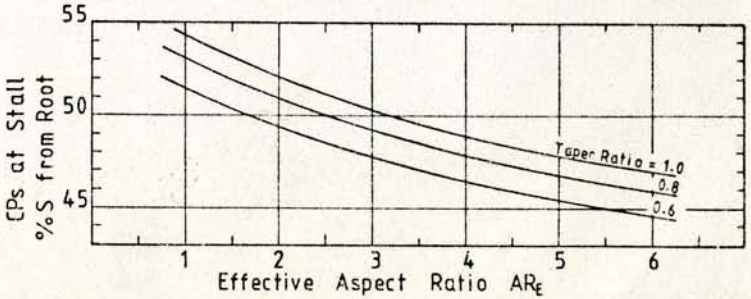

Fig. 6g CENTRE OF PRESSURE (SPANWISE):
ALL-MOVABLE RUDDERS

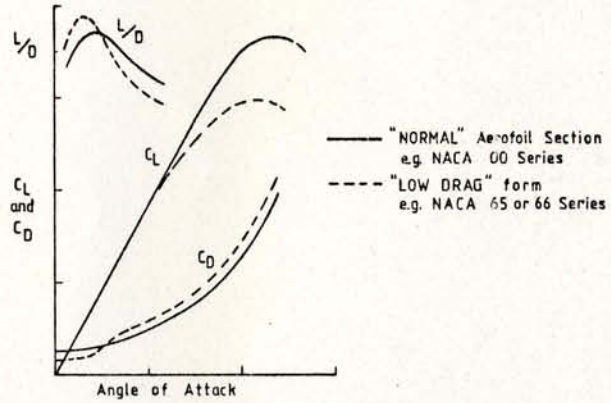

Fig. 7 COMPARISON BETWEEN "NORMAL" AND "LOW DRAG" SECTION CHARACTERISTICS

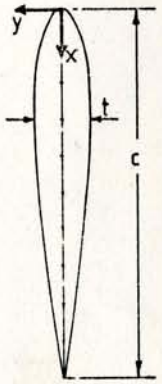

X %C from L.E.	y / max. t/2
0	0
1.25	0.316
2.50	0.436
5.0	0.592
7.5	0.700
10.0	0.780
15	0.891
20	0.956
25	0.990
30	1.000
40	0.967
50	0.862
60	0.761
70	0.611
80	0.437
90	0.241
95	0.134
100	0.021
Nose Radius = 110 $[t/c]^2$ % C	

NACA 00 SERIES

Fig. 8 OFFSETS FOR SUITABLE RUDDER SECTION

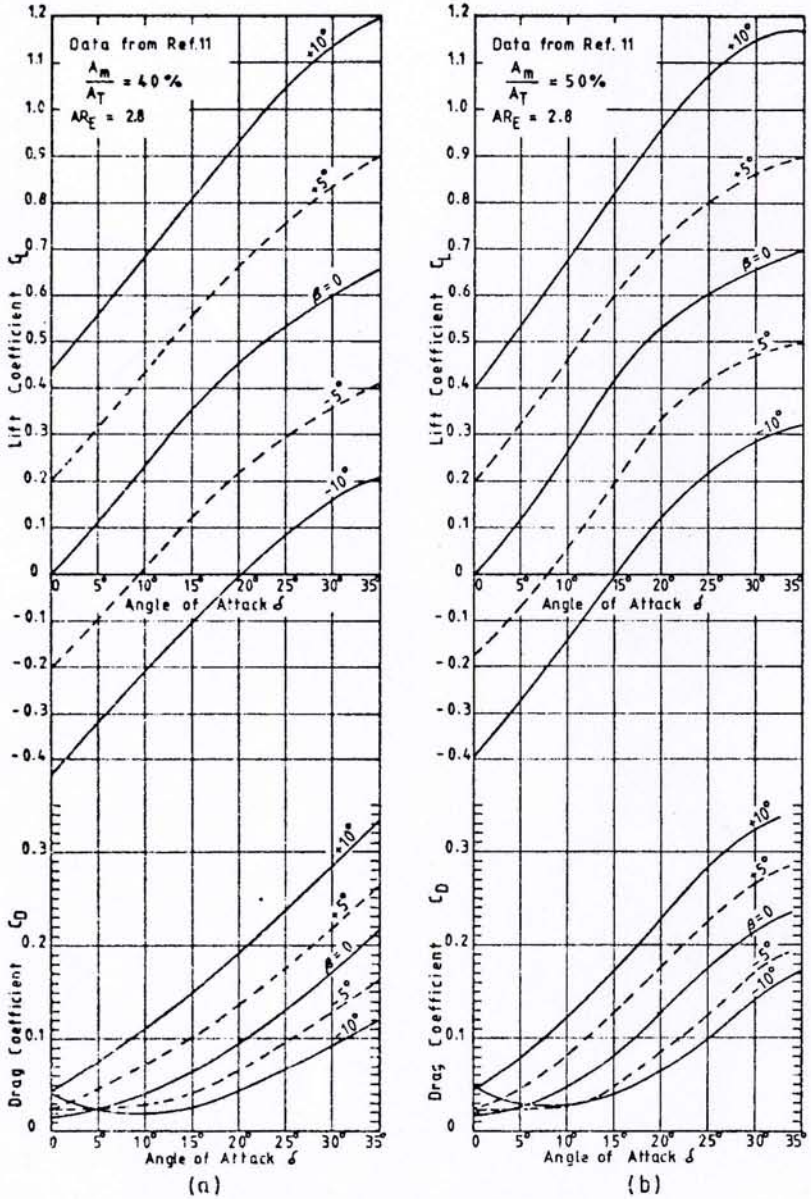

Fig. 9 SKEG RUDDER CHARACTERISTICS

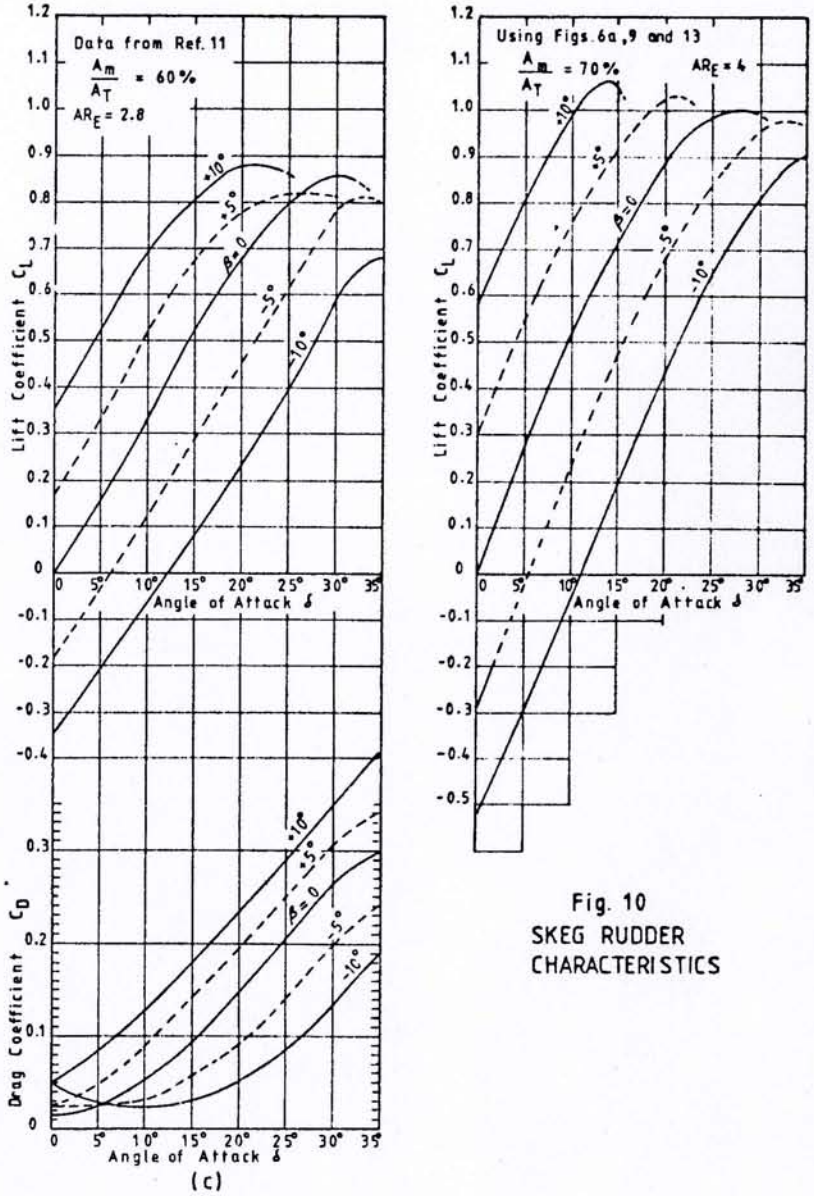

Fig. 10
SKEG RUDDER
CHARACTERISTICS

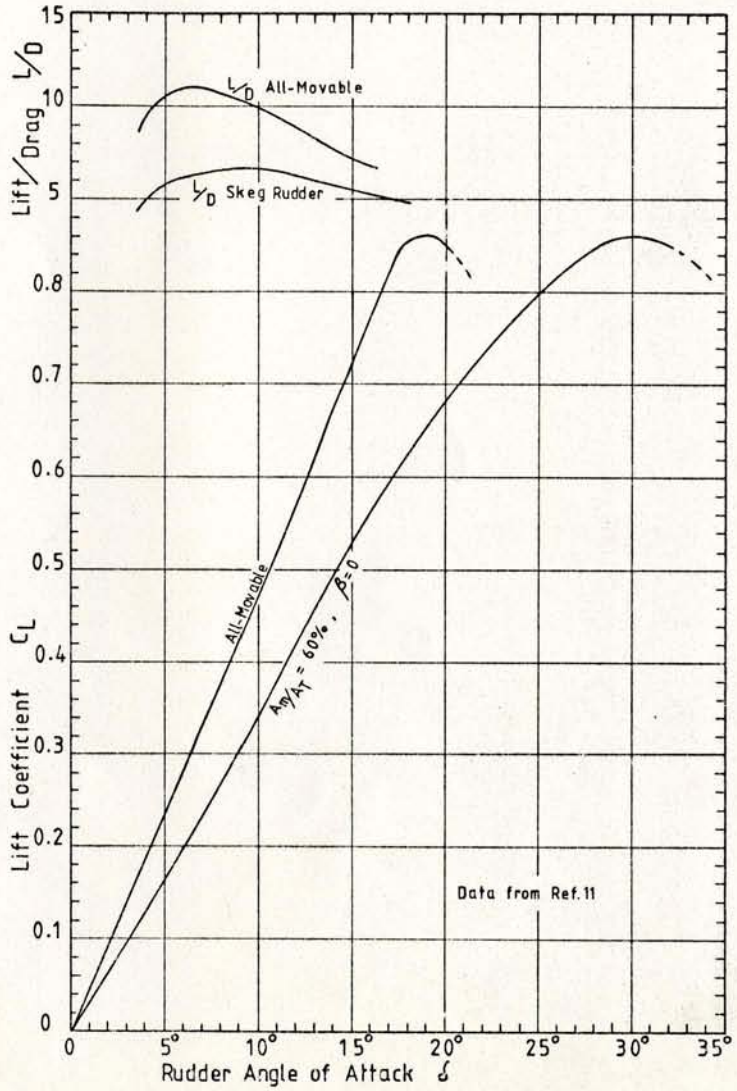

Fig. 11 COMPARISON BETWEEN ALL-MOVABLE AND SKEG RUDDER CHARACTERISTICS

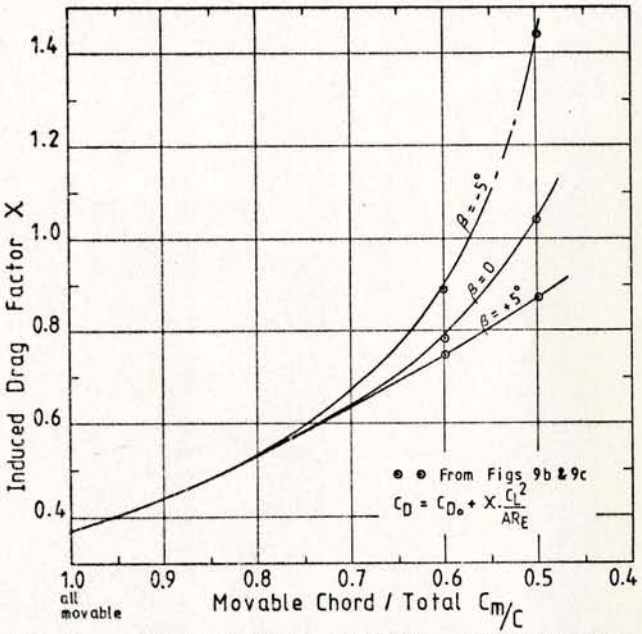

Fig. 12 INDUCED DRAG FACTOR - SKEG RUDDERS

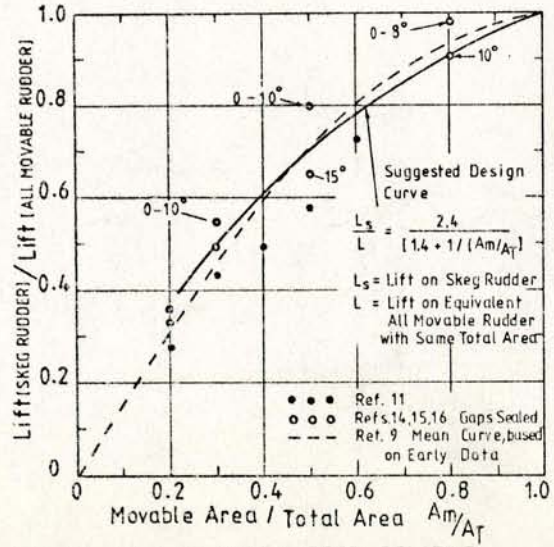

Fig. 13 LIFT OF SKEG RUDDER RELATIVE

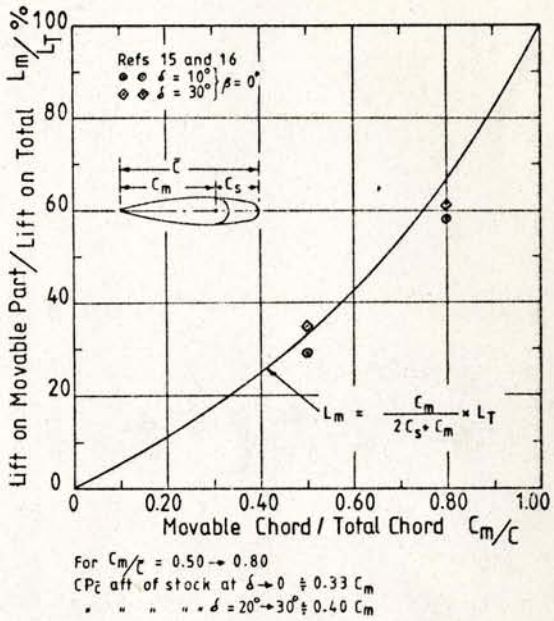

For C_m/c = 0.50 → 0.80
$CP_{\bar{c}}$ aft of stock at δ → 0 ≒ 0.33 C_m
" " " " δ = 20° → 30° ≒ 0.40 C_m

Fig. 14 LIFT OF MOVABLE PART OF SKEG RUDDER RELATIVE TO TOTAL

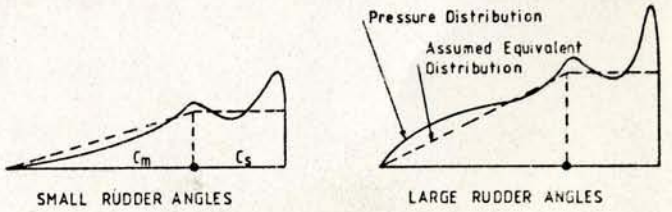

Fig. 15 TYPICAL CHORDWISE PRESSURE DISTRIBUTIONS FOR SKEG RUDDER [β = 0]

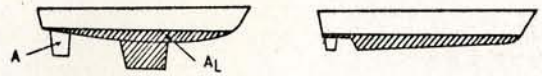

A = Rudder Area = sum of rudder areas if more than one rudder fitted
A_L = Immersed Lateral Area (based on static condition)

SAILING YACHTS and MOTOR SAILERS

$A = 0.07 A_L$ to $0.11 A_L$

$A = 0.085 A_L$ [for $A_L \neq 40 m^2$] to $0.105 A_L$ [for $A_L \neq 5 m^2$] – – – Ref. 23

LOW SPEED POWER CRAFT

$A = 0.03 A_L$ to $0.05 A_L$

SEMI-DISPLACEMENT and PLANING CRAFT

$A = 0.03 A_L$ to $0.04 A_L$ (A_L in static condition)

Following mean curve is based on data from Refs. 3 and 26 for satisfactory existing craft (rudders) operating in slipstream of propeller(s)

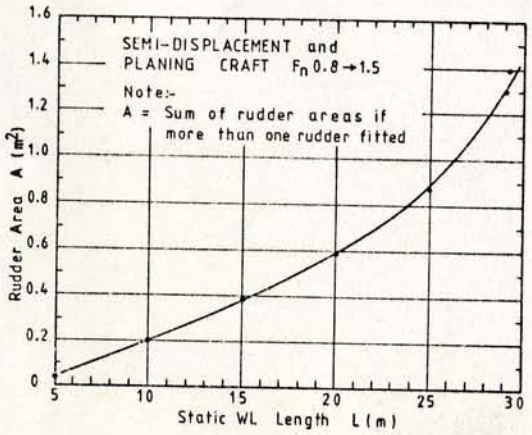

Fig. 16 TYPICAL RUDDER AREAS FOR SMALL CRAFT

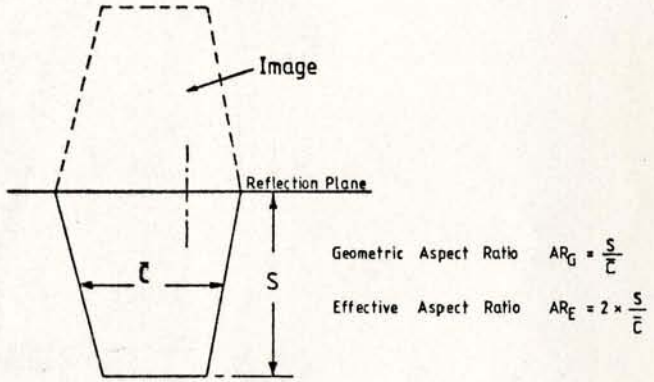

Fig. 17 INFLUENCE OF REFLECTION PLANE ON ASPECT RATIO

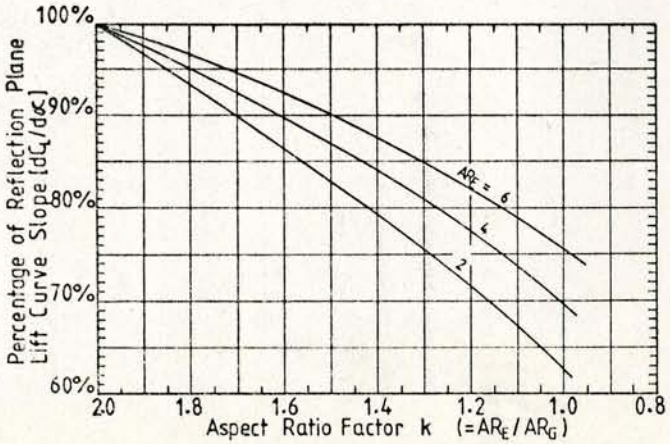

Fig. 18 RELATIONSHIP BETWEEN LIFT CURVE SLOPE AND ASPECT RATIO FACTOR (based on Eqt. 2)

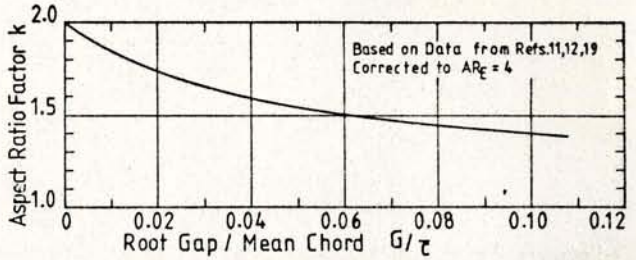

Fig. 19 INFLUENCE OF RUDDER ROOT GAP ON EFFECTIVE ASPECT RATIO

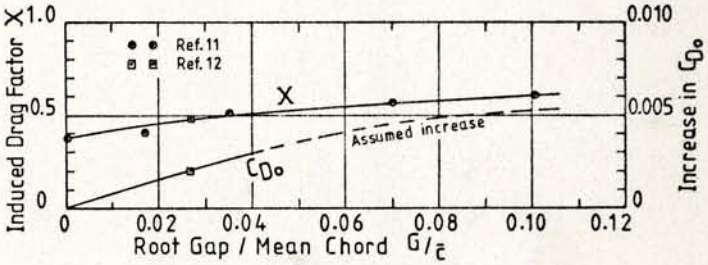

Fig. 20 INFLUENCE OF RUDDER ROOT GAP ON DRAG COEFFICIENT

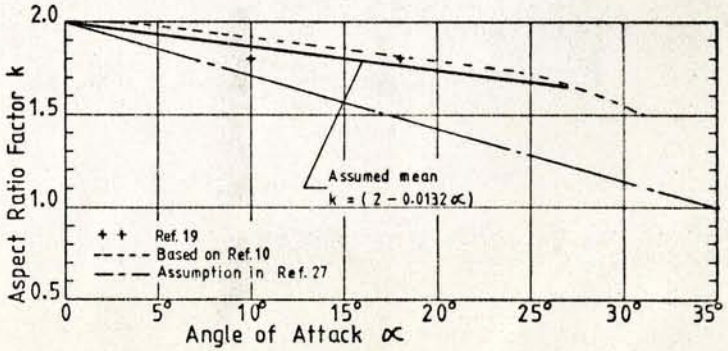

Fig. 21 INFLUENCE OF HULL SHAPE ON EFFECTIVE ASPECT RATIO

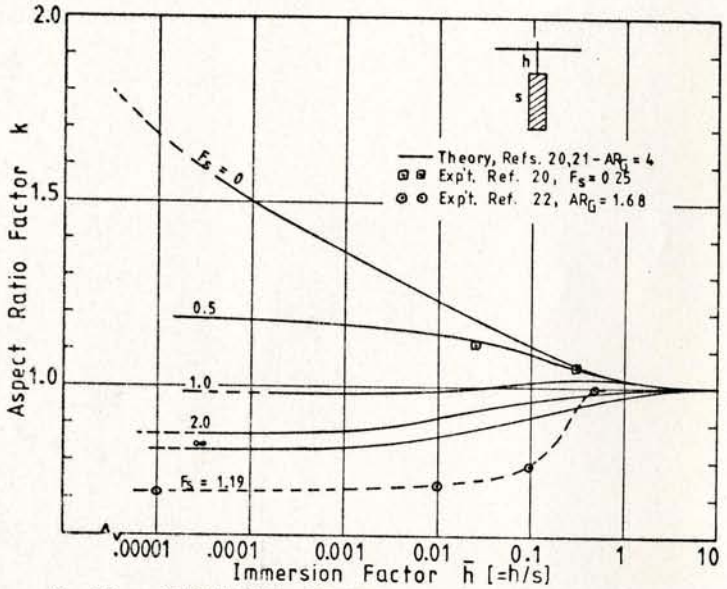

Fig. 22a INFLUENCE OF SPEED AND IMMERSION ON ASPECT RATIO FACTOR

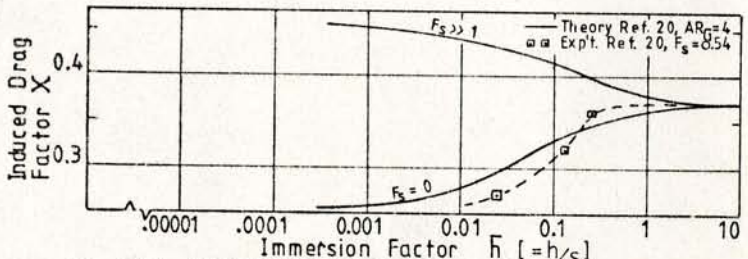

Fig 22b INFLUENCE OF SPEED AND IMMERSION ON INDUCED DRAG FACTOR

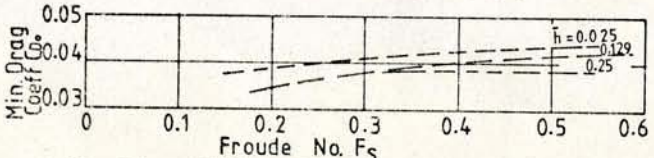

Fig 22c INFLUENCE OF SPEED AND IMMERSION ON MINIMUM DRAG COEFFICIENT

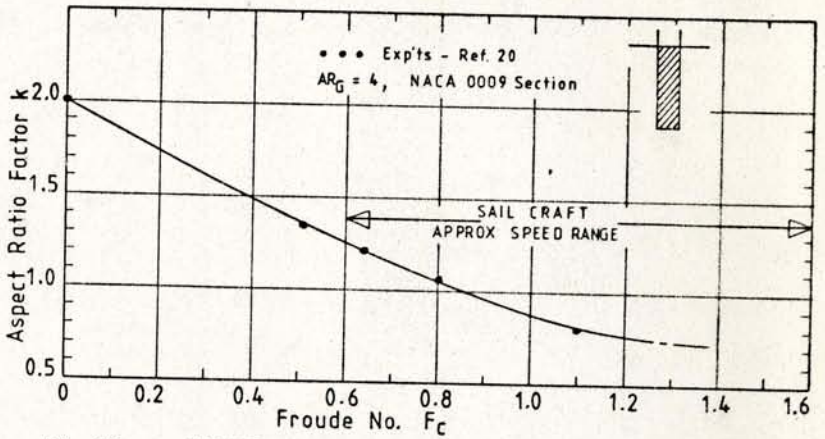

Fig. 23a INFLUENCE OF SPEED ON ASPECT RATIO FACTOR - SURFACE PIERCING CASE

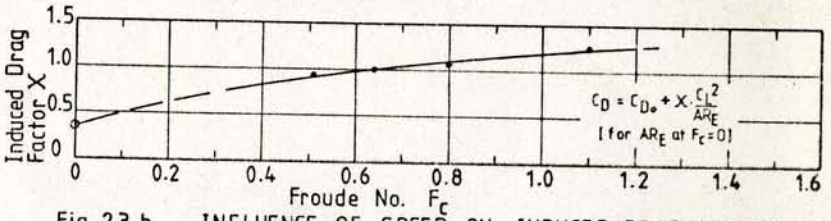

Fig. 23b INFLUENCE OF SPEED ON INDUCED DRAG FACTOR - SURFACE PIERCING CASE

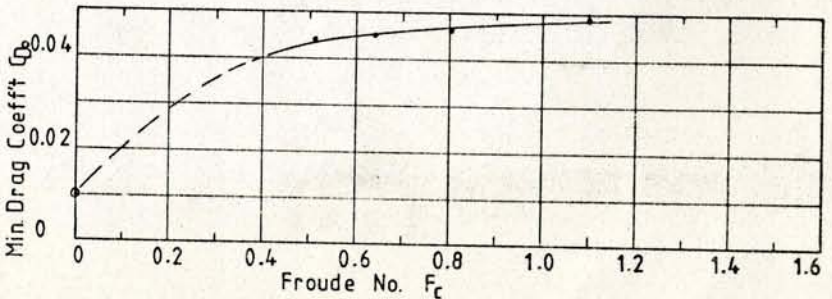

Fig. 23c INFLUENCE OF SPEED ON MINIMUM DRAG

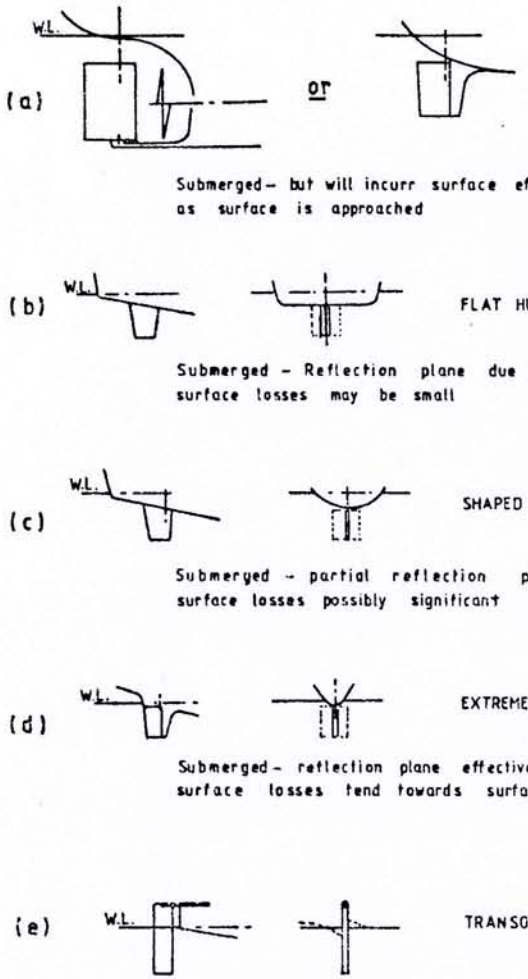

Fig. 24 TO ILLUSTRATE FREE SURFACE EFFECTS

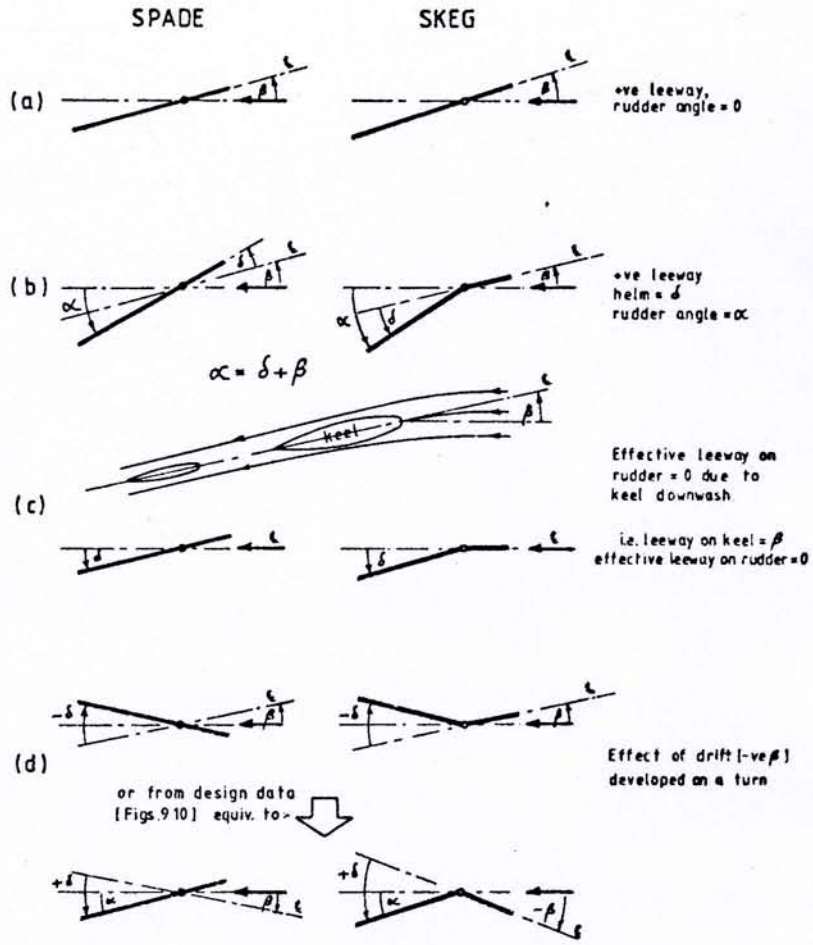

Fig. 25 COMPARISON BETWEEN EFFECTIVE ANGLE OF ATTACK ON SPADE (ALL-MOVABLE) AND SKEG RUDDERS

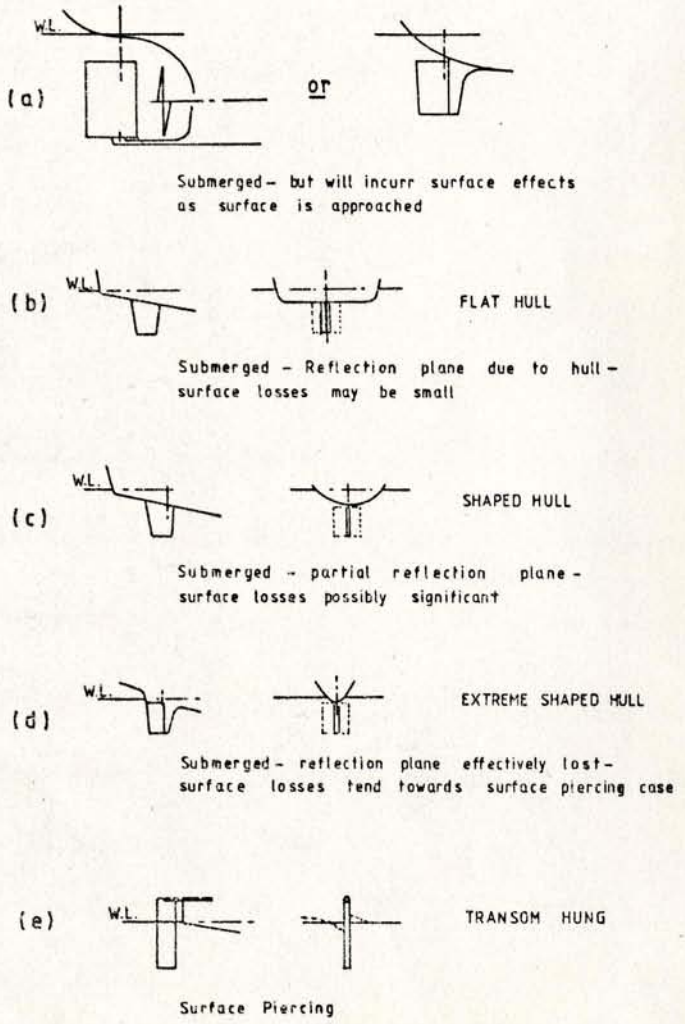

Fig. 24 TO ILLUSTRATE FREE SURFACE EFFECTS

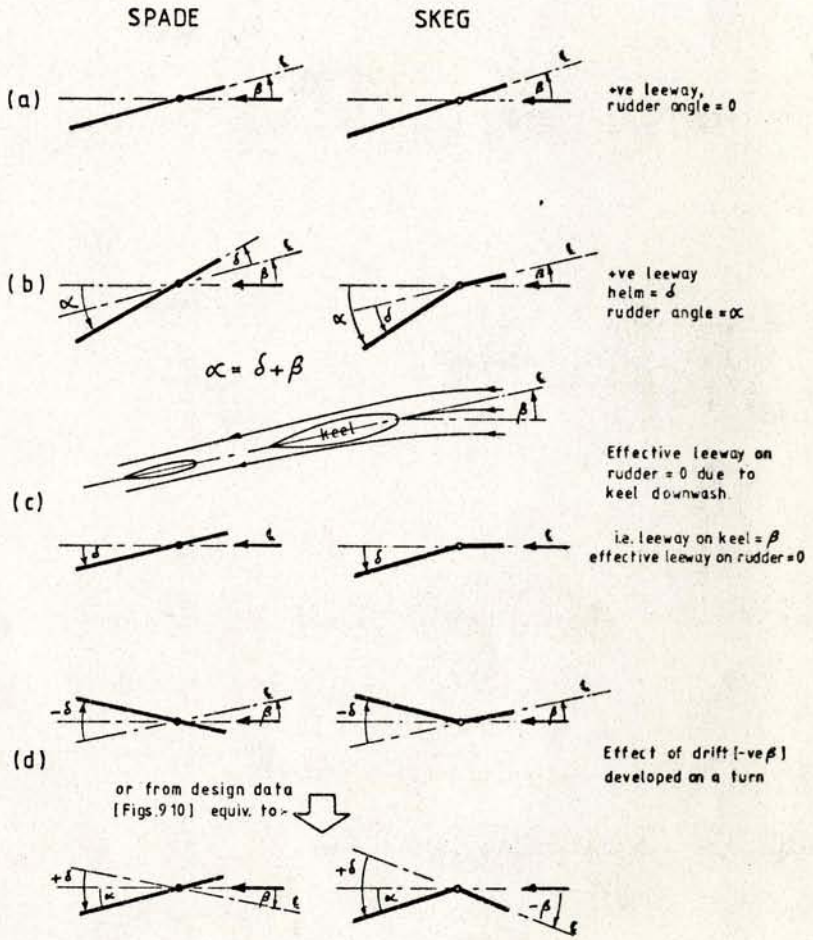

Fig. 25 COMPARISON BETWEEN EFFECTIVE ANGLE OF ATTACK ON SPADE (ALL-MOVABLE) AND SKEG RUDDERS